Journal of Quantitative Spectroscopy & Radiative Transfer 111 (2010) 2160–2184

Contents lists available at ScienceDirect

Journal of Quantitative Spectroscopy & Radiative Transfer

journal homepage: www.elsevier.com/locate/jqsrt

IUPAC critical evaluation of the rotational–vibrational spectra of water vapor. Part II
Energy levels and transition wavenumbers for $HD^{16}O$, $HD^{17}O$, and $HD^{18}O$

Jonathan Tennyson [a,*], Peter F. Bernath [b], Linda R. Brown [c], Alain Campargue [d], Attila G. Császár [e], Ludovic Daumont [f], Robert R. Gamache [g], Joseph T. Hodges [h], Olga V. Naumenko [i], Oleg L. Polyansky [j,a], Laurence S. Rothman [k], Robert A. Toth [c], Ann Carine Vandaele [l], Nikolai F. Zobov [j], Sophie Fally [m], Alexander Z. Fazliev [i], Tibor Furtenbacher [e], Iouli E. Gordon [k], Shui-Ming Hu [n], Semen N. Mikhailenko [i], Boris A. Voronin [i]

[a] *Department of Physics and Astronomy, University College London, London WC1E 6BT, UK*
[b] *University of York, York, UK*
[c] *Jet Propulsion Laboratory, California Institute of Technology, Pasadena, CA, USA*
[d] *Université Joseph Fourier, Grenoble, France*
[e] *Loránd Eötvös University, Budapest, Hungary*
[f] *Université de Reims Champagne-Ardenne, Reims, France*
[g] *University of Massachussets, Lowell, MA, USA*
[h] *National Institute of Standards and Technology, Gaithersburg, MD, USA*
[i] *V. E. Zuev Institute of Atmospheric Optics, Russian Academy of Sciences, 1, Academician Zuev square, 634021 Tomsk, Russia*
[j] *Institute of Applied Physics, Russian Academy of Sciences, Nizhny Novgorod, Russia*
[k] *Harvard-Smithsonian Center for Astrophysics, Cambridge, MA, USA*
[l] *Institut d'Aéronomie Spatiale de Belgique, Brussels, Belgium*
[m] *Université Libre de Bruxelles, Brussels, Belgium*
[n] *Laboratory of Bond-Selective Chemistry, University of Science and Technology of China, Hefei 230026, China*

ARTICLE INFO

Keywords:
Water vapor
Transition wavenumbers
Atmospheric physics
Energy levels
MARVEL
Information system
Database
W@DIS
Infrared spectra
Microwave spectra
$HD^{16}O$
$HD^{17}O$
$HD^{18}O$

ABSTRACT

This is the second of a series of articles reporting critically evaluated rotational–vibrational line positions, transition intensities, pressure dependences, and energy levels, with associated critically reviewed assignments and uncertainties, for all the main isotopologues of water. This article presents energy levels and line positions of the following singly deuterated isotopologues of water: $HD^{16}O$, $HD^{17}O$, and $HD^{18}O$. The MARVEL (measured active rotational–vibrational energy levels) procedure is used to determine the levels, the lines, and their self-consistent uncertainties for the spectral regions 0–22 708, 0–1674, and 0–12 105 cm^{-1} for $HD^{16}O$, $HD^{17}O$, and $HD^{18}O$, respectively. For $HD^{16}O$, 54 740 transitions were analyzed from 76 sources, the lines come from spectra recorded both at room temperature and from hot samples. These lines correspond to 36 690 distinct assignments and 8818 energy levels. For $HD^{17}O$, only 485 transitions could be analyzed from three sources; the lines correspond to 162 MARVEL energy levels. For $HD^{18}O$, 8729 transitions were analyzed from 11 sources and these lines correspond to 1864 energy levels. The energy levels are checked against ones determined from accurate variational nuclear motion computations employing exact

* Corresponding author.
E-mail address: j.tennyson@ucl.ac.UK (J. Tennyson).

doi:10.1016/j.jqsrt.2010.06.012

kinetic energy operators. This comparison shows that the measured transitions account for about 86% of the anticipated absorbance of $HD^{16}O$ at 296 K and that the transitions predicted by the MARVEL energy levels account for essentially all the remaining absorbance. The extensive list of MARVEL lines and levels obtained are given in the Supplementary Material of this article, as well as in a distributed information system applied to water, W@DIS, where they can easily be retrieved. In addition, the transition and energy level information for $H_2{}^{17}O$ and $H_2{}^{18}O$, given in the first paper of this series [Tennyson, et al. J Quant Spectr Rad Transfer 2009;110:573–96], has been updated.

1. Introduction

The water molecule is the most abundant polyatomic molecule in the universe and the single most important species for controlling the Earth's climate. Thus, the spectrum of water is both one of the most important and one of the most thoroughly studied.

The first 14 authors of this article form a Task Group under the auspices of the International Union of Pure and Applied Chemistry (IUPAC) with the aim of constructing a database of water transitions from experiment and theory, with individual tasks described in Table 1 of the first paper in this series [1], henceforth known as Part I. Given the nature of water spectroscopy [2], this database will concentrate on the pure rotational and rotation–vibration transitions of water which we consider simultaneously on an equal basis. This paper is the second in a series presenting our evolving methods for collecting and analyzing the experimental and quantum chemical spectroscopic information as well as our validated data advocated for deposition in databases. In Part I, we derived energy levels and transition wavenumbers for the water isotopologues $H_2{}^{17}O$ and $H_2{}^{18}O$. This was done using the measured active rotational–vibrational energy levels (MARVEL) protocol of Furtenbacher et al. [3–5], which was refined during Part I to allow for the treatment of larger datasets and to perform a significant amount of checking in order to minimize errors and inconsistencies in the initial experimental transition data.

In this work we apply MARVEL to the $HD^{16}O$, $HD^{17}O$, and $HD^{18}O$ isotopologues of the water molecule. $HD^{16}O$, singly deuterated water, has a fractional abundance in the earth's atmosphere, compared to $H_2{}^{16}O$, of about 0.0003 (note that the natural $HD^{17}O/H_2{}^{17}O$ and $HD^{18}O/H_2{}^{18}O$ abundances have a similar, about 3×10^{-4} value). Even though a trace species, atmospheric absorption by HDO can be significant. This is particularly true for $HD^{16}O$ since some of its absorption spectrum, unlike that of $H_2{}^{17}O$ and $H_2{}^{18}O$, is significantly shifted from that of $H_2{}^{16}O$. Observation of atmospheric HDO spectra has long been used on both Earth [6] and other planets [7,8] as a proxy to understand their climatic evolution. Atmospheric HDO spectra are also being extensively observed because of the information they provide on the transport of water vapor into the stratosphere [9,10]. Abundance of HDO relative to H_2O can vary significantly; the proportion of HDO on Venus, for example, is over 100 times that of the terrestrial value [11].

Astrophysical observations of HDO are also potentially important [9]. Deuterium was formed in the first few minutes after the Big Bang. As D is burnt rapidly in stellar interiors, the abundance of D has been decreasing since this time. Deuterium burns in objects with masses greater than about 13 times that of Jupiter, which is one way of defining the boundary between a brown dwarf and a planet. Observations of HDO in the atmospheres of such objects, which are cool enough to be largely molecular but hot by terrestrial standards, could be the key to a deuterium test [12] that would distinguish between planets and other sub-stellar objects. In the cold interstellar medium fractionation effects become important leading to an expected over-abundance of HDO [13].

Table 1
Experimental sources recalibrated for the three isotopologues of HDO during the course of this work.

Tag	Range (cm^{-1})	Calibration factor	Shift[a] (cm^{-1})	Median[b]	Original standard
78KaKaKy [43]	151–420	1.000005413	+0.0013	293	
86FlCaMaGu [52]	1125–1890	0.99999977	−0.00035	29	[47]
91RiSmDeBe [58]	1176–1650	0.99999998	−0.00003[c]	49	[132]
83Guelachv [47]	1191–1740	0.99999977[d]	−0.00035	45	[133]
89OhSa [55]	6384–6596	0.99999893	−0.0069	23	[134]
99HuLiHeCh [70]	12 525–12 912	1.000000819[e]	+0.0104	7	[135]
00NaBeCaSc [75]	13 165–13 500	0.999999452[f]	−0.0073		

[a] Shift of the middle wavenumber value of the range (new–old).
[b] Indicates that half of the energy levels involved in the transitions in the given source are part of at least this many measured and validated transitions.
[c] This shift is within the original precision of about 0.00006 cm^{-1}.
[d] The same calibration factor was determined in [130].
[e] A very similar calibration factor was determined in [100].
[f] This is the only ICLAS measurement which was recalibrated as part of the present study.

Astronomical applications of water spectra therefore require spectral data appropriate for very low temperatures up to stellar temperatures of about 3000 K.

As emphasized in Part I, a distinguishing feature of the present series of IUPAC-sponsored studies is the joint utilization of all available experimental and the best theoretical line and level data, with a long-term aim to create a complete linelist for all water isotopologues. While determination of a complete linelist is outside the scope of present-day experiments, it can be determined by means of sophisticated first-principles quantum mechanical computations. Consequently, as long as experiments have a higher precision than even the most advanced computations that can be performed for a molecule of the size of water, the complete linelist will necessarily contain accurate experimental data and less accurate computational data. MARVEL-type efforts help to (a) replace as many computed lines as possible with their experimental counterparts, (b) validate and ideally reduce the uncertainty with which a transition has been determined, and (c) facilitate the assignment of experimental spectra.

2. Methods, input data, and data treatment

The methods employed in this study for collecting and critically evaluating experimental transition wavenumbers and their uncertainties and for inverting the wavenumbers in order to obtain the best possible energy levels with uncertainties are based on the MARVEL procedure [3–5] involving the iterative robust reweighting scheme [14]. During a MARVEL analysis we simultaneously process *all* the available assigned experimental lines and the associated energy levels for the chosen isotopologue. MARVEL is not designed to determine any new energy levels. However, from the MARVEL energy levels obtained one can determine transitions whether they have been measured or not. The reweighting scheme means that uncertainties for certain selected transitions are changed (increased) during iterations of the MARVEL procedure. After cleansing of the database and applying the iterative robust reweighting algorithm of MARVEL, a database is created containing self-consistent and correctly assigned transitions and the seemingly best possible related uncertainties supported by the database. Energy levels, and their uncertainties, determined from these transitions are in harmony with the measured transitions and their (adjusted) uncertainties.

The first step in the MARVEL procedure is to split the transition data into spectroscopic networks (SN). SNs contain all interconnecting rotational–vibrational energy levels supported by the grand database of the transitions. For HDO, as there is no nuclear spin symmetry, the vast majority of the data forms a single SN. Other interconnecting but unattached transition networks are designated as floating networks (FSNs) or, in the case of a single transition with no energy level in common with any of the other transitions in the compilation, orphans (ORPs).

For $HD^{16}O$ there is a considerable number of experimental data sources available [15–109].In particular, we note that a number of hot $HD^{16}O$ spectra [64,82,86,106] are included in the above list. Hot spectra are usually considerably richer in transitions but have significantly larger uncertainties and a higher chance of misassignment than spectra recorded at room temperature. As expected, there is a much smaller number of publications reporting measured and assigned transitions for $HD^{17}O$ [61,110, 111] and $HD^{18}O$ [42,51,61,102,108,110,112–115].

Tables 2–4 provide, for each data source, experimental information related to the spectra of $HD^{16}O$, $HD^{17}O$, and $HD^{18}O$, respectively. The number of originally measured (A) and validated (V) transitions for each data source is given there, as well. Due to the large number of related experimental studies, a nearly continuous coverage has been achieved for $HD^{16}O$ up to 22 800 cm^{-1} but not for the other two isotopologues. As modern measurements of pure rotational transitions at microwave frequencies ($< 30\,cm^{-1}$) are very scarce, the microwave transitions were mostly obtained from early works and are limited in number. Conversely, early infrared measurements, such as that by Benedict et al. [29], have largely been superceded by more recent and more accurate measurements and were therefore largely omitted from the final compilation.

To be included in our tabulation, data sources must include original experimental line positions with uncertainties, line assignment, and information on the experimental conditions under which the experimental data were recorded. The latter data are summarized in the column "Physical conditions" in Tables 2–4. In each case the data source is identified with a tag, as specified in Part I, based on year of publication and the names of the authors.

Abundance is a particular issue with spectra of HDO. Since a pure sample of HDO would partially disproportionate to H_2O and D_2O, it is not possible to record spectra of pure HDO. In practice, 50% HDO is normally the best that can be achieved. The presence of significant quantities of H_2O and D_2O in any HDO sample means that a good knowledge of spectra of these species is a prerequisite for analyzing spectra of HDO. Furthermore, it is very difficult to get complete spectral coverage for HDO since some transitions are obscured by strong lines associated with H_2O or D_2O.

Most of the spectra were obtained by Fourier transform spectroscopy (FTS), which gives a wide spectral coverage from the microwave region to the near ultraviolet. In order to detect weak lines, FTS spectrometers have been equipped with long multipass cells. Absorption path lengths as large as 433 and 1804 m have been achieved with the cells available at Kitt Peak and Reims, respectively, providing a large number of observed transitions, mostly in the near infrared (NIR) region.

Laser-based methods, such as CRDS (cavity ringdown spectroscopy) and ICLAS (intracavity laser absorption spectroscopy), are limited to certain spectral regions depending on the availability of tunable laser sources. These techniques have specific advantages in terms of sensitivity and spectral resolution, which make them particularly suitable for the characterization of spectral regions with weak absorption features. This is why

Table 2
Data sources and their characteristics for $HD^{16}O$ (see Section 2.8 for comments[a]).

Tag	Range (cm^{-1})	Trans. A/V	Physical conditions					Comments
			T (K)	p (hPa)	Abun.	Rec.	L (m)	
62TrBe [32]	0.016–0.028	2/2	RT			SMM		(2a)
55WeBeHe [27]	0.016–0.102	6/1	RT			SMM		(2b)
53BeWe [21]	0.027–0.101	5/4	RT			SMM		(2c)
54PoSt [26]	0.19–0.90	7/7	RT			MS		(2d)
68VeBlDy [35]	0.286	1/1	RT			BMS		(2e)
53Crawford [24]	0.295	3/1	RT			SMM		(2f)
57Posener [30]	0.343	1/1	RT			SMM		(2g)
64ThKrLo [33]	0.343	1/1	RT			BMS		(2h)
67BlVeDy [34]	0.343	1/1	RT			BMS		(2i)
49Strandbe [18]	0.343–1.676	3/3	RT	29.33		SMM		(2j)
71LaBeSt [39]	0.35–2.24	9/9	RT					
70BeSt [37]	0.682–5.344	3/3	RT			MS		
46ToMe [15]	0.744	1/1	RT					(2k)
53JeBiMa [22]	0.830–0.89	2/2	RT		50%	MS		(2l)
49Mcafee [17]	0.90–0.90	1/1						
56ErCo [28]	1.674–8.052	6/6	RT			MS		
70StBe [36]	1.730–8.872	11/11	RT			MS		
73ClBeKlRo [40]	2.93–8.872	6/0	RT			SMM		
71DeCoHeGo [38]	2.93–25.13	36/36	RT		50%	TMS		
93GoFeDeDu [62]	7.54–8.07	3/3	100–600	0.013–1.3		CCC		(2m)
87BaAlAlPo [54]	7.680–11.527	3/1	1000			MW		(2n)
84MeDeHe [49]	0.39–33.67	32/32				MW		(2o)
76FlGi [42]	15.51–39.37	20/13	RT	13.3	50%	FS		(2p)
85Johns [51]	20–339	225/225		1.33		FTS		(2q)
78KaKaKy [43]	152–419	60/60	RT	0.53–5.3		FTS	0.50	(2r)
95PaHo [63]	171–498	335/335	295	0.5	50%	FTS		(2s)
03JaTeBeZo [86]	381–3932	11 503/11 184	1770	3.33	25%	FTS		(2t)
99Toth [72]	657–2066	749/748	296	0.6–6.8	40–47%	FTS		(2u)
93Tothb [61]	969–1892	1267/1265	297	0.4–21.2	10–49%	FTS	0.25–2.39	(2v)
86FlCaMaGu [52]	1125–1890	1253/1252	RT	7.6		FTS		(2w)
91RiSmDeBe [58]	1176–1650	266/266	294–297	≥ 1.3	$\geq 1\%$	FTS	1.21	(2x)
83Guelachv [47]	1191–1740	428/420	RT	13–1000	Nat	FTS		(2y)
00SiBeMaMa [76]	1480	1/1	RT	0.2–4.6	50%	L	2.7	(2z)
82PaCaFlGu [44]	2237–3114	1902/1892	295.8 ± 1	1.3–8.9	$\geq 10\%$	FTS	20.18–60.18	(2aa)
82ToGuBr [46]	2503–3099	575/574	296	21.4		FTS	0.25	(2bb)
92RiSmDeBe [59]	2576–2726	48/48	294–297	> 1.3	$> 1\%$	FTS	1.21	(2cc)
83ToBr [48]	3289–4369	1002/1000	296	16.07	48%	FTS		(2dd)
73CaFlGuAm [41]	3702–3789	8/7				FTS		
07JeDaReTy [101]	4200–6599	3088/3074	293 ± 2	2.7–22.7	Nat	FTS		
97Tothb [66]	4719–5781	1824/1816	RT	1.3–22.7	50%	FTS	0.25–73	(2ee)
07MiWaKaCa [103]	5964–7015	274/274		1.5–20		CRDS		(2ff)

Table 2 (*continued*)

Tag	Range (cm^{-1})	Trans. A/V	Physical conditions					Comments
			T (K)	p (hPa)	Abun.	Rec.	L (m)	
01UlHuBeOn [81]	6003–7064	2424/2384	RT	15.16	15–44%	FTS	64–87	(2gg)
97Tothc [67]	6003–7626	2590/2571	296	1.8–13	3–49.1%	FTS	2.39–73	(2hh)
09LiNaKaCa [108]	6076–6623	498/498				CRDS		(2ii)
04MaRoMiNa [91]	6131–6748	1695/1693	RT	22.3	Nat	CRDS		(2jj)
89OhSa [55]	6384–6596	596/576	RT	12	50%	L		(2kk)
91SaTaIrNa [57]	6563–6565	3/3	RT	16.4	50%	L	1.0	(2ll)
05ToTe [92]	7428–8759	171/163	292 ± 3			FTS		(2mm)
04NaVoHu [90]	7500–8194	1415/1401	296	10	50%	FTS	87	
01HuHeZhWa [83]	8246–9063	899/873	RT	10	50%	FTS	105	(2nn)
05UlHuBeZh [95]	8713–9598	1000/996	296	18.4		FTS	123	
06NaLeCa [98]	9099–9645	1999/1900	RT	18	50%	ICLAS	$\leq 23\,400$	
08PeSoSi [106]	9387–9450	232/220		13–26				
05ToNaZoSh [93]	9758–10 797	212/201	294.4	20.08	Nat	FTS	≤ 600	(2oo)
00WaHeHuZh [79]	9648–10 201	654/649	RT	10	50%	FTS	123	(2pp)
03BeNaCa [87]	9628–10 111	1416/1361	RT	26.3	50%	ICLAS	$\leq 35\,000$	(2qq)
08ToTe [107]	9879–13 901	133/87	RT	9–23	Nat	FTS	5–800	(2rr)
04NaHuHeCa [89]	10 110–12 215	1827/1787	RT	15	50%	FTS	105	(2ss)
97VoFaPlRi [65]	10 631–10 690	17/16				OPO		
08LiHo [105]	10 693–10 738	4/4	RT		Nat	CRDS		(2tt)
07MaToCa [102]	11 809–12 126	64/56	RT	26.7		ICLAS	4800–14 000	(2uu)
05CaVaNa [96]	11 645–12 329	1615/1542	RT	18.4	50%	ICLAS	9000	
07VoNaCaCo [100]	11 750–22 708	3481/3378	291	6.7	48%	FTS	600	(2vv)
08NaVoMaTe [104]	12 144–13 159	1330/1300	RT	18.4	50%	ICLAS	$\leq 24\,000$	
99HuLiHeCh [70]	12 525–12 912	243/219				FTS		(2ww)
98LaPeSiZh [68]	12 720–12 912	121/120	300	17	50%	PAS		(2xx)
10NaBeLeCa [109]	13 021–14 113	2078/2019	RT	18.4	Various	ICLAS	24 000	
00NaBeCaSc [75]	13 165–13 500	676/572	RT	18.4	50%	ICLAS	$\leq 15\,000$	
99NaBeCa [71]	13 579–14 033	459/391	298	26.7	50%	ICLAS	$\leq 15\,000$	
00NaCa [73]	14 986–15 340	470/405	RT	17.3	50%	ICLAS	$\leq 12\,000$	
00CaBeNa [74]	16 304–18 349	400/348	RT		50%	ICLAS		
01JeMeCaCo [80]	16 344–22 703	507/488	291.1	13.07	47%	FTS	603.32	(2yy)
00BeNaCa [78]	16 542–17 054	309/287	RT	17.3	50%	ICLAS	12 000, 19 500	
90ByKaKoNa [56]	16 746–17 013	237/203	RT	20	50%	PAS		

[a] The tags listed are used to identify experimental data sources throughout this paper. The range given represents the range corresponding to wavenumber entries within the MARVEL input file of the particular water isotopologue and not the range covered by the relevant experiment. Uncertainties of the individual lines can be obtained from the Supplementary Material. Trans. = transitions, with A = number of assigned transitions in the original paper, V = number of transitions validated in this study. T = temperature (K), given explicitly when available from the original publication, with RT = room temperature. p = pressure (hPa). Abun. = abundance (%) of the given isotopologue in the gas mixture, with Enr = enriched and Nat = natural abundance. Rec. = experimental technique used for the recording of the spectrum, with SMM = Stark-modulated microwave spectrometer, L = different lasers, CCC = collisionally cooled cell, MC = microwave cavities, TMS = tunable microwave spectrometer, PAS = photo-acoustic spectrometer, and OPO = optical parametric oscillator.

Table 3
Data sources and their characteristics for $HD^{17}O$ (see Section 2.9 for comments[a]).

Tag	Range (cm^{-1})	Trans. A/V	Physical conditions					Comments
			T (K)	p (hPa)	Abun.	Rec.	L (m)	
78Lovas [110]	0.29–8.06	59/54	RT					(3a)
57StTo [111]	0.346	2/2	RT					(3b)
93Tothb [61]	1118–1674	424/422	RT			FTS		(3c)

[a] See footnote a to Table 2.

Table 4
Data sources and their characteristics for $HD^{18}O$ (see Section 2.10 for comments [a]).

Tag	Range (cm^{-1})	Trans. A/V	Physical conditions					Comments
			T (K)	p (hPa)	Abun.	Rec.	L (m)	
78Lovas [110]	0.20–8.06	27/27	RT					(4a)
76FlGi [42]	16.4–39.9	17/16	RT					(4b)
06ZeBaKuRi [112]	16.73	1/1	RT					(4c)
85Johns [51]	24.9–219.8	191/191	RT					(4d)
06LiDuSoWa [138]	1090–7609	4931/4858		13.07	0.8%	FTS	105	(4e)
93Tothb [61]	1125–1804	704/702	RT	1.60	0.86%	FTS	2.4	(4f)
05Toth [113]	2517–3018	354/352	RT	2.00	10.5%	FTS	2.4	(4g)
09MiTaPuSt [114]	4205–10 717	1012/999	RT	3–19	Nat	FTS	600–1800	(4h)
10MiTaDaJe [115]	5600–8744	299/298	296	3–13	Nat	FTS	600	(4i)
09LiNaKaCa [108]	6000–6722	1101/1099	299	0.13–13	0.028	CRDS		(4j)
07MaToCa [102]	11 638–12 105	92/92	RT	26.7		ICLAS	4800–14 000	(4k)

[a] See footnote a to Table 2.

extensive investigations with laser-based methods were mostly limited to transparency windows or to the visible region. In spite of the small natural abundance of even $HD^{16}O$, part of the data were obtained from spectra recorded with water in natural abundance.

2.1. Pre-MARVEL validation

As for Part I, the experimental databases assembled for the three HDO isotopologues were checked for transcription problems or problems characterizing the original data source. The following checks were made apart from the trivial checks for formatting incompatibilities and looking for entries with zero uncertainties. The dataset of transitions was searched looking for cases where the K_a + K_c sum, where K_a and K_c are the usual asymmetric top rigid rotor quantum numbers, had a value different from J or J + 1, where J is the rotational quantum number. We also searched for obvious duplications in the dataset and a warning was issued if this happened. Overall, fewer problems were detected for the HDO isotopologues than observed for $H_2{}^{17}O$ and $H_2{}^{18}O$ in Part I [1].

2.2. Assignment, labels

It is a requirement of the MARVEL protocol that the dataset contains a single unique assignment to label both the lower and the upper states involved in each transition. In this work we retain the order of vibrational labels applicable to $H_2{}^{16}O$ for HDO, i.e., ν_1, ν_2, and ν_3 stand for the OD stretching, bending, and OH stretching quantum numbers, respectively, and they provide the vibrational label (ν_1 ν_2 ν_3). Note that in some works, such as Ref. [116], ν_1 and ν_3 are reversed. We use the standard asymmetric top quantum numbers [J K_a K_c] or $J_{K_aK_c}$ to label the rotational states. Thus, the rotation–vibration levels of each isotopologue are identified uniquely by six labels altogether.

Before processing the published transition data we checked, as thoroughly as possible, whether the assignments were correct and consistent. Rovibrational labels, which can be used for checking the (ν_1 ν_2 ν_3) [J K_a K_c] labels, can be taken from computations based on the use of an effective Hamiltonian (EH). In the EH approach, all vibrational states are combined in the polyads of interacting states based on the ratio between the harmonic frequencies ω_1, ω_2, and ω_3. For $HD^{16}O$, ω_1 is at 2823 cm^{-1}, very close to twice ω_2, which is at 1444 cm^{-1}, while ω_3, at 3887 cm^{-1}, lies much higher. This structure leads to a series of well isolated (0 0 $n\nu_3$) vibrational states, whose energy levels can be easily fitted, and, consequently, labeled within the EH approach. At the same time, the coincidence of ω_1 and $2\omega_2$, and the strong centrifugal distortion effects inherent in HDO, result in strong and numerous anharmonic resonances. These result in the formation of the resonance polyads which often include highly excited bending states. This complicates proper EH analysis and therefore inhibits the process of labeling for many of the high-lying energy levels. We note that to run MARVEL successfully such

labels simply have to be self-consistent; the MARVEL process itself says nothing about the physical basis of the labels [117].

Validation of the assignments attached to the observed transitions was performed as follows. All transitions were examined for consistency of the upper levels derived from combination difference (CD) relations. This method is a simple and powerful tool for the assignment of rovibrational spectra; however, it is often inapplicable to weak transitions because of the incompleteness of the set of observed transitions. All the transitions associated with a given rotational level of the (000) vibrational ground state have been considered for combination differences. At this stage, conflicting labels could be easily traced and corrected. This step was helped considerably by the availability of results from variational nuclear motion computations [118]. Where necessary, labels were changed assuming similar increases in rotational energies as a function J and K_a for similar vibrational states with the same v_2 quantum number as well as quasi-degeneracy of rotational levels with K_a close to J or K_a equal to 0 or 1. In the end, consistent labeling has been established for all the assignments considered. We recommend that the labeling provided in this paper should be generally adopted, although in case of strongly perturbed energy levels there is some remaining ambiguity.

2.3. Uncertainties

Within the MARVEL protocol reasonable estimates for the accuracy of the observed transitions must be provided. Despite the adjustments by the robust reweighting scheme, false uncertainties attached to the transitions can noticeably deteriorate the accuracy of the MARVEL energy levels.

In the majority of the data sources proper experimental uncertainties are not given for each transition. Often only the general accuracy of the data for the region investigated is provided. For a few publications we were forced to estimate the experimental uncertainties. As no values were presented in the original source, these were based on average values characteristic of the experimental setup exploited in the measurement.

For further important adjustment of the uncertainties of the transitions see Sections 2.6 and 2.8.

2.4. Variational validation

As an independent validation of the experimental transition wavenumbers and the derived MARVEL energy levels, systematic comparisons were made with the results of state-of-the-art variational nuclear motion computations. For this comparison the newly computed VTT $HD^{16}O$ linelist [118] was used; this linelist was computed using the spectroscopically determined HDO potential energy hypersurfaces of Yurchenko et al. [119], the so-called CVR dipole moment surface [120], and the DVR3D nuclear motion program suite [121].

When variational results are used for validation, we can rely on a well-known feature of such calculations: the smooth and slow variation of obs–calc residuals for the energy levels of a particular vibrational state having the same K_a and increasing J values [122]. The longest obs–calc sequences could be investigated for the hot spectra, where transitions involving J as high as 30 have been detected. Examples of the obs–calc deviations for the energy levels of the (000) state with K_a = 1–5 are shown in Fig. 1. The obs–calc residuals for levels with a given K_a but different K_c increase as J increases, hindering the assignment of the dense observed spectrum without detailed consideration of these near degeneracies.

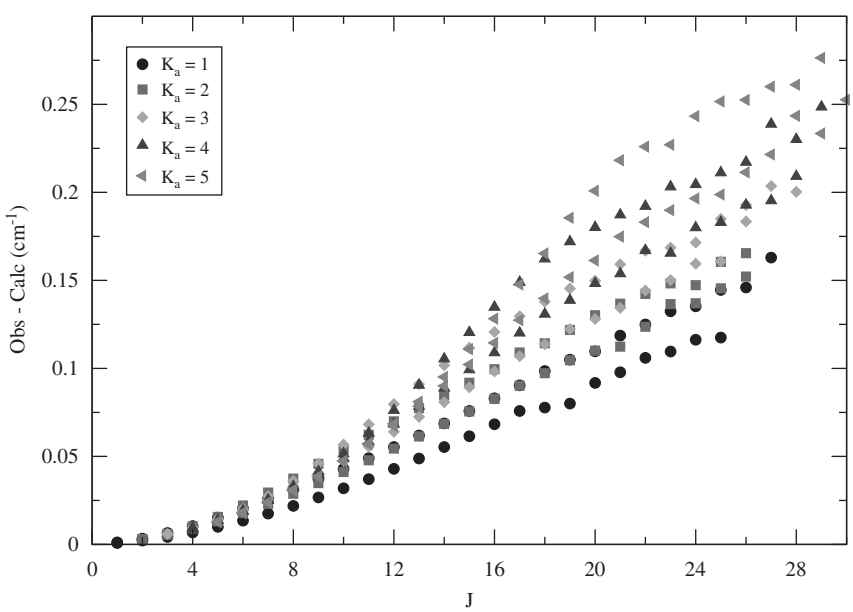

Fig. 1. Residuals of "observed" (MARVEL) minus calculated (VTT [118]) energy levels of $HD^{16}O$ for the ground vibrational state and K_a between 1 and 5.

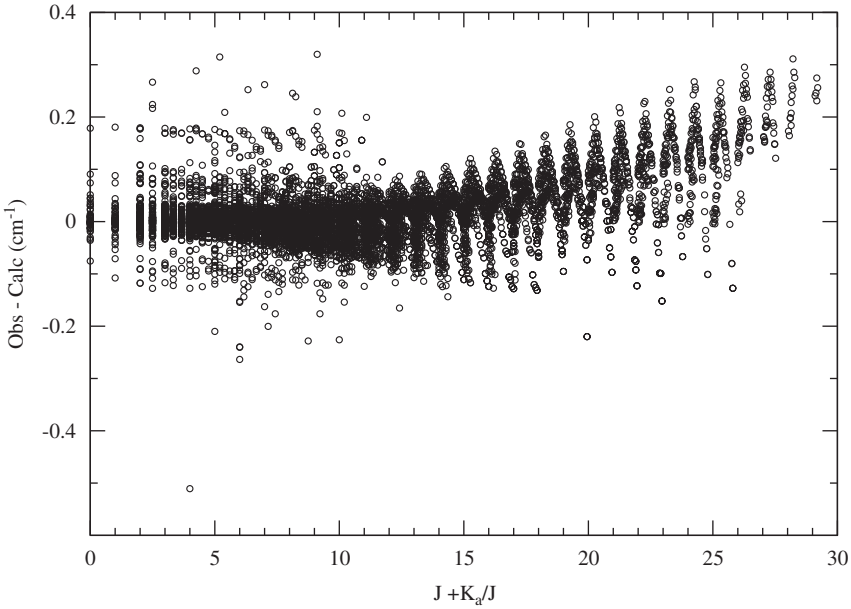

Fig. 2. Residuals of "observed" (MARVEL) minus calculated (VTT [118]) for all the energy levels of $HD^{16}O$ derived in this work.

The trends in obs–calc for the highly excited vibrational states are not particularly smooth as they can be strongly perturbed by nearby states. Examples of perturbations of the obs–calc trend due to resonance interactions can be observed in Fig. 2. Cases with erratic obs–calc trends were additionally checked to see whether the calculated energy level set includes the resonance partner, whose energy level has to be close to the level under investigation and whose quantum numbers should satisfy the conventional Coriolis-, Fermi-, or Darling–Dennyson-type resonance interaction rules, or some combination of them. We stress that the so-called HEL (highly excited local) resonances [123], which do not obey conventional resonance selection rules and can involve energy levels with a large difference in the v_2 bending quantum number, are especially strong in HDO due to the close coincidence between the ω_1 and $2\omega_2$ harmonic frequencies [100].

Those transitions which involved a MARVEL energy level that did not have a matching variational counterpart within the obs–calc trend established for the corresponding vibrational state were "deleted" from the input to MARVEL (by adding a minus sign in front of the wavenumber) and the MARVEL process was repeated until all MARVEL levels had variational counterparts within the appropriate obs–calc trend; possible resonance distortions of these trends were also taken into account. The final, accepted obs–calc values vary in magnitude from 0.01 up to 0.32 cm^{-1} depending on the vibrational state and the J and K_a values. A comparison of the experimental (MARVEL) and variational [118] energy levels is given in Fig. 3. For transitions removed at this stage, see the appropriate comments in the footnotes supplementing Tables 2–4. Levels which the Task Group considers to be marginally reliable were retained but are flagged in the appropriate entry (see the Supplementary Material).

2.5. Hot transitions

Unsurprisingly, the hardest levels to validate came from the hot transitions observed and assigned in 03JaTeBeZo [86], due to the high density of both predicted and observed transitions and the possibility of transitions to a given upper level originating from lower (sometimes unknown) levels belonging to different vibrational states. During the process of comparing the observed and calculated energy levels it was discovered that 03JaTeBeZo often gave only one assignment to transitions involving quasi-degenerate lower and upper levels. This impeded proper evaluation of the second component of the quasi-degenerate pair and, consequently, led to the disconnection of many experimental energy levels which are connected to these second components. To solve this problem, the second components of the quasi-degenerate transitions omitted in 03JaTeBeZo were added to the data based on predictions of the VTT variational linelist. Experimental transitions were considered to be degenerate if their variational centers coincided within 0.015 cm^{-1}, since the smallest difference between experimentally observed lines in 03JaTeBeZo was always at least 0.02 cm^{-1}. By this means about 1600 extra line assignments were added to the 03JaTeBeZo list (marked with D, see the Supplementary Material).

For the validation procedure we also used the unpublished experimental linelist of hot HDO emission spectra recorded by Mellau in the 400–900 cm^{-1} region

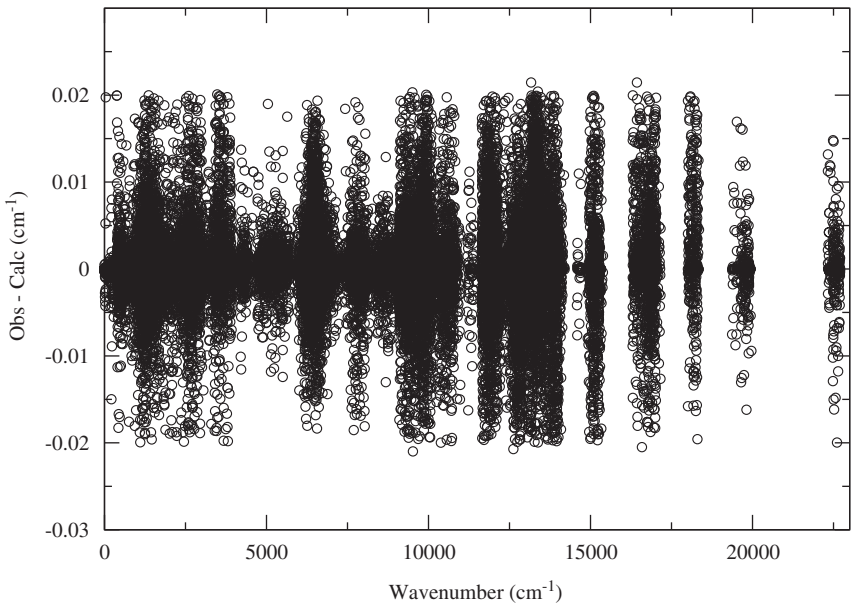

Fig. 3. Differences between the measured transition wavenumbers and those calculated using the MARVEL energy levels derived in this work for $HD^{16}O$.

[64]. Due to peculiarities of the hot spectrum assignment, deleting one unconfirmed experimental transition may lead to the loss of many experimental energy levels derived in 03JaTeBeZo. For this reason we assigned 65 transitions using the unassigned lines from the experimental linelist attached to 03JaTeBeZo (for details see the Supplementary Material).

2.6. Recalibration

As discussed in Part I, the absolute accuracies of different datasets vary, producing systematic offsets in the observed line positions. In massive compilations which gather measurements obtained over decades, these differences can arise partly because calibration standards improve over time. In the early 1980s, advanced techniques produced frequency measurements that became the dominant standards for infrared spectroscopy with reported accuracies between 3×10^{-7} and $2\times10^{-5}\,cm^{-1}$: CO_2 at 10 μm [124], the P(7) line of CH_4 at 3.34 μm [125], and the 2–0 band of CO at 2.3 μm [126]. Using these frequency standards, transitions of other gases were recalibrated but often with lesser precision ($1\times10^{-4}\,cm^{-1}$). With FTS data, such corrections are easily made just by applying a multiplicative factor obtained as a ratio of the new to the old positions. Water, being ubiquitous in spectrometer chambers and having many strong bands throughout the infrared, was reinvestigated against the then-exceptional quality frequencies [124–126]. For example, the best prior v_2 band line positions near 6 μm [47] were altered by a factor of 0.99999977 [127]. Later, newer technological developments resulted in calibration standards in the near-infrared, such as C_2H_2 near 1.5 μm [128] and atomic potassium near 0.77 μm [129].

During the course of this study it became apparent that there are several sources of HDO data which might suffer from calibration problems. The sources identified include 78KaKaKy [43], 83Guelachv [47], 93Tothb [61], 86FlCaMaGu [52], 89OhSa [55], 91RiSmDeBe [58], 99HuLiHeCh [70], and 99Toth [72]. It is straightforward to determine multiplicative calibration factors with MARVEL by minimizing the root-mean-square (rms) deviation between the observed transitions with wavenumbers scaled with a given calibration factor and those produced by MARVEL from the energy levels. This minimization was performed sequentially for all the problematic data sources; Table 1 gives the calibration factors we determined for cases where our analysis gave a result which differed significantly from unity. For the sources 91RiSmDeBe, 93Tothb, and 99Toth the MARVEL analysis suggests that no recalibration is needed or possible; thus, these transitions were not altered. For 78KaKaKy, 83Guelachv, 86FlCaMaGu, and 89OhSa the experimental FTS data were adjusted using the calibration factors determined. Only the recalibrated results were used in the final data analysis.

Improvement of the ICLAS data via recalibration was attempted only in one case here [75]. This is despite the fact that there are known calibration problems with some of the ICLAS data [100]. These arise because different calibration lines are used for every few cm^{-1}, making it difficult to determine a unique calibration factor for the whole region covered or employ a constant shift value.

From time-to-time, the available frequency standards are re-evaluated producing new recommendations (e.g., [130,131]). The last composite review [130] was performed 15 years ago. Thus, we must be mindful that on-going advancements in frequency measurements may later reveal the need for further recalibration of the HDO data collected here.

2.7. Post-MARVEL validation

While data handling within the MARVEL process is performed as automatically as possible, for a number of transitions, which proved to be clear outliers by combination difference relations, the experimental uncertainties were increased manually (see footnotes to Tables 2–4) by a process we call post-MARVEL validation.

This extra validation and the subsequent adjustment was done when the energy of an upper rotational–vibrational state deviated far more from the corresponding mean value established by the lower MARVEL energy levels plus the transition wavenumbers than the stated experimental uncertainty. The MARVEL protocol can make similar adjustments automatically if the error associated with a transition is an outlier and all the data have similar accuracy. However, a problem arises if an erroneously small experimental uncertainty is attached to what is actually a much less accurate experimental datum, the same level is involved in several measurements, and other transitions in the combination difference relations, though are consistent, have formally much larger uncertainties. In this case the MARVEL energy level will be determined by the formally most accurate transition which, in fact, represents an outlier.

For HDO, all data declared to have very high accuracy, such as those from 07VoNaCaCo [100], 07JeDaReTy [101], 97Tothc [67], and 07MiWaKaCa [103], were subject to post-MARVEL checks. In this context we note that sometimes the experimental uncertainty attached to a line in the original source reflects the quality of the line profile fit rather than the real accuracy with which the wavenumber was determined.

This validation was not performed in Part I. Thus, in the active update of the data of $H_2{}^{17}O$ and $H_2{}^{18}O$ presented in the Appendix of this paper the energy levels were subjected to a post-MARVEL validation.

2.8. Comments on the data sources for $HD^{16}O$ given in Table 2

(2a) 62TrBe: A spectrometer containing a Stark-modulated microwave coaxial cavity was used to measure nine hyperfine components of two rotational transitions, the $3_{31}\rightarrow 3_{30}$ and $5_{42}\rightarrow 5_{41}$ lines at 487 and 825 MHz, respectively. The hyperfine components are not included in the MARVEL analysis.

(2b) 55WeBeHe: The apparatus of Ref. [21] was used for the measurements. Frequencies and absorption coefficients of six transitions between 486 and 3045 MHz are reported. Frequencies of five of these have been previously measured in Ref. [21].

(2c) 53BeWe: The spectrometer employed Stark modulation and operated at frequencies lower than 600 MHz.

(2d) 54PoSt: The number of original measured line frequencies is 5. In addition, the authors reproduce three frequencies from two other measurements: one transition from 49Mcafee [17] and two transitions from "Microwave Spectroscopy Laboratory, Research Laboratory of Electronics, Massachusetts Institute of Technology (unpublished work)". Note also that one of the five frequencies of this source (8577.7 ± 0.1 MHz, the $7_{44}\rightarrow 7_{43}$ transition) was previously reported in 53BuSt [23] but without an uncertainty.

(2e) 68VeBlDy: The hyperfine structure of one rotational line, at 8577.812 MHz, was investigated with a beam maser spectrometer. The wrong rotational assignment, $7_{43}\rightarrow 7_{45}$, of the reported line was changed to the correct $7_{44}\rightarrow 7_{43}$. Measured and calculated values of the hyperfine coupling constants are reported but not used here.

(2f) 53Crawford: Three observed lines are reported in this paper. The 8577.80 ± 0.08 and 8837.22 ± 0.12 MHz transitions correspond to $HD^{16}O$ transitions $7_{44}\rightarrow 7_{43}$ and $10_{56}\rightarrow 10_{55}$, respectively; only the latter was included in the final transitions file. The third one at 8884.83 MHz is neither an HDO nor a D_2O line.

(2g) 57Posener: Fine structure of the $2_{21}\rightarrow 2_{20}$ rotational line reported previously in Ref. [18] was examined by Stark modulation spectroscopy. Five components were observed but not employed here.

(2h) 64ThKrLo: Nine hyperfine components of the $2_{21}\rightarrow 2_{20}$ rotational transition have been reported at about 10 278.2455 MHz with a beam maser spectrometer.

(2i) 67BlVeDy: The hyperfine structure of the $2_{21}\rightarrow 2_{20}$ rotational line at 10 278.246 MHz was investigated with a beam maser spectrometer. Measured values of the hyperfine coupling constants as well as the electric quadrupole coupling tensor are reported but not employed here.

(2j) 49Strandbe: Four rotational absorption transitions, $2_{21}\rightarrow 2_{20}$, $3_{22}\rightarrow 3_{21}$, $4_{14}\rightarrow 3_{21}$, and $5_{33}\rightarrow 5_{32}$, have been observed and identified using the Stark effect. The frequencies of the first three transitions are given in the paper. The last one was reported earlier in Ref. [16].

(2k) 46ToMe: Frequency of one pure rotational transition, $5_{33}\rightarrow 5_{32}$, was reported. The frequency value, 22 309 ± 5 MHz, is rather far from the more precise values reported later for the same transition.

(2l) 53JeBiMa: The frequencies of four rotational lines have been observed in microwave absorption. One of them, 26 880.47 ± 0.1 MHz, was observed previously [17]. Two lines at 24 884.85 ± 0.1 (A) and 26 880.47 ± 0.1 (B) MHz correspond to the $HD^{16}O$ transitions $8_{45}\rightarrow 8_{44}$ and $6_{24}\rightarrow 7_{17}$, respectively. The two unassigned lines at 30 182.57 ± 0.1 (C) and 30 778.62 ± 0.1 MHz (D) correspond to $D_2{}^{16}O$ transitions $9_{63}\rightarrow 8_{72}$ and $9_{64}\rightarrow 8_{71}$, respectively. Stark spectra of all four lines and Zeeman spectra of the A and B lines were recorded.

(2m) 93GoFeDeDu: Three microwave transitions of $HD^{16}O$, reported previously by 84MeDeHe [49], were broadened by H_2, N_2, O_2, and He for $100 \le T \le 600$ K. Measurements made at 10 mTorr of $HD^{16}O$ and about 40 broadening gas pressures up to 1 Torr.

(2n) 87BaAlAlPo: Three rotational transitions in the (0 1 0) vibrational state are reported. Only one of them, $4_{14}\rightarrow 3_{21}$ at 230 427.34 MHz, is confirmed. The other transitions, $6_{33}\rightarrow 7_{26}$ at 334 018.30 MHz and $5_{24}\rightarrow 4_{13}$ at 345 795.94 MHz, have very large discrepancies as compared to the expected frequency values (about 335 138 and 346 620 MHz, respectively).

(2o) 84MeDeHe: 32 newly reported rotational transitions complemented by transitions reported previously [40].

(2p) 76FlGi: Among the 20 $HD^{16}O$ transition only 13 were validated. The seven excluded transitions have differences between reported and expected frequency values larger than 0.02 cm^{-1}.

(2q) 85Johns: Far infrared pure rotational spectra of six water isotopologues were recorded with pressures less than 1 Torr (only for wavenumbers below 30 cm^{-1} was the pressure raised to 2 Torr) to minimize pressure shifts and broadening. The list of $HD^{16}O$ transitions includes 84 MW frequencies from 84MeDeHe [49] and 212 measured line positions which correspond to 225 transitions. The experimental uncertainty was raised to 0.0002 cm^{-1} instead of 0.00005 cm^{-1} stated originally.

(2r) 78KaKaKy: Three spectra were recorded but only for one spectrum (150–320 cm^{-1}, p = 1.8 Torr) was the $HD^{16}O$ abundance greater than natural. The experimental accuracy has been estimated in the original source to be better than 0.001 cm^{-1} under favorable conditions. After recalibration, 65% (39 lines) of the 65 observed transitions agree with the MARVEL transitions within the declared experimental accuracy of 1.0×10^{-3} cm^{-1}. All original experimental uncertainties equal to 5×10^{-4} were changed to 1.5×10^{-3}.

(2s) 95PaHo: Pure rotational spectra of ^{16}O water isotopic species were measured with a high resolution FTS in order to obtain better calibration line positions in the 110–500 cm^{-1} spectral region.

(2t) 03JaTeBeZo: Fourier transform emission spectra analyzed together with line positions obtained in 01PaBeZoSh [82]. Supplementary data for this article contain a list of 32 399 records which correspond to 31 645 unique line positions. Ten thousand six hundred and fifty seven rotation–vibration assignments are given in this line list. Seven hundred and forty five of them are labeled with "D_2O" or "H_2O", probably they are HDO lines blended by "D_2O" and "H_2O", respectively. About 1600 transitions which represent the second components of quasi-degenerate transitions, omitted in the original source, have been added to the list, as well as 65 newly assigned transitions. After validation of the spectrum, a list of 11 182 transitions has been included into the final transitions file. Of the 11 182 validated transitions, only 67.9% (7592 lines) agree with the MARVEL transitions within the declared experimental uncertainty of 1.0×10^{-3} cm^{-1}, suggesting that the true experimental accuracy of the line positions can be lower than declared. Furthermore, all original experimental uncertainties of 5.0×10^{-3} have been lowered to 2.0×10^{-3} cm^{-1}.

(2u) 99Toth: High-resolution Fourier-transform spectra were analyzed to obtain line positions and strengths of over 6000 transitions of HDO and D_2O. For $HD^{16}O$, line positions and strengths of pure lines and of rovibrational bands (0 1 0)–(0 0 0), (0 2 0)–(0 1 0), and (1 0 0)–(0 1 0) are reported. Of the 749 observed transitions reported for $HD^{16}O$, 95.5% (715 lines) agree with the MARVEL transitions within the declared experimental uncertainty of 1×10^{-4} cm^{-1}. There is an asymmetry in the obs–MARVEL deviations with respect to the zero line: there are 276 positive and 473 negative deviations. This asymmetry concerns mainly the 1000–1360 cm^{-1} region. A calibration factor could not be determined.

(2v) 93Tothb: Fourier transform spectra in the v_2 band region have been recorded for the determination of line positions and line intensities of $HD^{16}O$, $HD^{17}O$, and $HD^{18}O$. Of the 1267 lines assigned to $HD^{16}O$, 94.8% (1201 lines) agree with MARVEL transitions within the declared experimental uncertainty of 1.2×10^{-4} cm^{-1}. An asymmetry is detected in the obs–MARVEL deviations with respect to zero line: there are 412 positive and 855 negative deviations. A calibration factor could not be determined as it does not seem to be constant for the whole spectral region considered.

(2w) 86FlCaMaGu: Four spectra recorded between 1040 and 1900 cm^{-1} with different pressures and mixtures of D_2O and H_2O in order to obtain v_2 line positions of $HD^{16}O$. After recalibration of the experimental spectrum, 99.3% (1244 lines) of the 1253 observed transitions agree with the MARVEL transitions within 2.0×10^{-4} cm^{-1}, compared to the stated experimental uncertainty of 4.0×10^{-4} cm^{-1}. The experimental uncertainties of the lines between 1210 and 1890 cm^{-1} were decreased from 4×10^{-4} to 2×10^{-4} cm^{-1}. As the applied calibration factor was not constant throughout the spectrum, there is a remaining asymmetry in the obs–MARVEL deviations with respect to the zero line: there are 764 positive and 489 negative deviations. In the region below 1200 cm^{-1} most part of the observed–MARVEL deviations are negative, with a root-mean-square agreement of 3.6×10^{-4} cm^{-1}. Uncertainties that belong to the 1210–1890 cm^{-1} interval were changed from 4.0×10^{-4} to 2.0×10^{-4} cm^{-1}.

(2x) 91RiSmDeBe: Measured Lorentz-broadening and pressure-shift coefficients by air, N_2, and O_2 are presented for the 266 v_2 $HD^{16}O$ lines. Twelve spectra were recorded at 0.0053 cm^{-1} resolution. Spectra with buffer gas were recorded at total sample pressures of about 200, 300, and 400 Torr. Spectra have been calibrated using 93Tothb [61] data, and then the experimental accuracy has been adopted in this study as 1.2×10^{-4} cm^{-1}, similar to that of 93Tothb. All 265 observed lines agree with MARVEL transitions within 7.4×10^{-5} cm^{-1}. An asymmetry in the obs–MARVEL deviations with respect to the zero line: there are 182 positive and 83 negative deviations. A calibration factor could not be determined with the technique employed in this study as it is not constant for the whole spectral region considered. Original experimental uncertainties of 5.0×10^{-4} cm^{-1} have been adjusted to 1.2×10^{-4} cm^{-1}.

(2y) 83Guelachv: Fourier transform spectra with absorption paths of 16, 24.17, 32.17, and 44.17 m. Due to a calibration problem the original reported transitions had to be scaled by a scale factor of 0.99999977 [130]. The MARVEL input file includes only the recalibrated transitions, with the original uncertainties. After recalibration of the spectrum, 95.1% (407 lines) of the 428 observed transitions agree with the MARVEL transitions with an rms deviation of 1.5×10^{-4} cm^{-1}, compared to an experimental uncertainty of 1.2×10^{-4} cm^{-1}, estimated as an average value of individual experimental uncertainties attached to every line. As the applied calibration factor was not constant throughout the spectrum, there is

a remaining asymmetry in the obs–MARVEL deviations with respect to the zero line: there are 151 positive and 277 negative deviations, with the most serious discrepancies in the 1400–1600 cm^{-1} region.

(2z) 00SiBeMaMa: A CO laser was used for observation of the saturated absorption dip of the nearby v_2 $5_{24}\rightarrow5_{15}$ line of $HD^{16}O$. The absolute frequency of this line was obtained as $1480.094038033 \pm 67\times10^{-9}\,cm^{-1}$ ($44\,372\,102.973 \pm 0.002$ MHz).

(2aa) 82PaCaFlGu: The $2v_2$ and v_1 bands of $HD^{16}O$ were analyzed using Fourier transform spectra of pure D_2O and of 90% H_2O–10% D_2O mixtures.

(2bb) 82ToGuBr: HDO gas samples obtained from different mixtures of H_2O and D_2O with concentrations of $HD^{16}O$ estimated as 50%, 48%, and 28%. For a number of lines the experimental uncertainties were adjusted from 4×10^{-3} to $4\times10^{-4}\,cm^{-1}$.

(2cc) 92RiSmDeBe: Absorption spectra recorded for measurements of Lorentz-broadening coefficients and pressure-induced line-shift coefficients of 48 lines in the v_1 band of HDO were recorded using the FTS of the Kitt Peak National Observatory. Gas samples were prepared by mixing distilled H_2O with 99.96 at% D_2O. Low pressure (<1.0 Torr) samples were mixed with samples diluted with high-purity N_2, O_2, or ultra zero air at total sample pressures of about 200, 300, and 400 Torr.

(2dd) 83ToBr: FTS spectra recorded by 82ToGuBr [46] [see comment (2bb)] were studied for line positions and strengths in the 3289–4369 cm^{-1} region.

(2ee) 97Tothb: The FTS of the Kitt Peak National Observatory was used for measuring $HD^{16}O$ spectra with absorption path lengths of 0.25, 2.39, 25, and 73 m. Of the 1824 observed transitions, 66.5% (1213 lines) agree with the MARVEL transitions with an rms deviation equal to the declared experimental uncertainty of $1.0\times10^{-4}\,cm^{-1}$. The measurement accuracy seems to be slightly overestimated.

(2ff) 07MiWaKaCa: Absorption spectra of natural abundance water vapor near the 5911.0–5922.5, 5926.0–5941.8, 5957.0–6121.6, and 6475.0–7015.6 cm^{-1} spectral regions. Pressure values on the order of 10–20 hPa were chosen in the 1.66 μm region and of about 1.5–2.0 hPa in the 1.455 μm region. Most of the original experimental uncertainties were increased, from 8.0×10^{-5} to $1.0\times10^{-3}\,cm^{-1}$.

(2gg) 01UlHuBeOn: The Bruker IFS 120 HR FTS of the University of Science and Technology (Hefei, China) was used to record two spectra: the first spectrum had a total pressure of 1516 Pa, 44% HDO and a path length of 87 m; the second spectrum had a total pressure of 1500 Pa, 15% HDO and a path length of 69 m. Transition data supplied by Hu. Of the 2424 observed transitions, 92.9% (2251 lines) agree with the MARVEL transitions with an rms deviation equal to the declared measurement accuracy of $2.0\times10^{-3}\,cm^{-1}$. There is an asymmetry in the observed–MARVEL deviations with respect to the zero line: there are 735 positive and 1689 negative deviations. A calibration factor for the whole spectral region covered could not be determined. For 60% of the reported transitions obs–MARVEL deviations are less than 0.001 cm^{-1}, confirming that the measurement accuracy is slightly better than declared.

(2hh) 97Tothc: Of the 2590 observed transitions, 61.8% (1600 lines) agree with the MARVEL transitions with an rms deviation equal to the declared experimental uncertainty of $1.0\times10^{-4}\,cm^{-1}$. The stated measurement accuracy seems to be slightly overestimated.

(2ii) 09LiNaKaCa: Absorption spectrum of ^{18}O enriched water was recorded using CW-CRDS and a series of fibered DFB lasers. The CRDS sensitivity allowed the detection of lines with intensity as low as 10^{-28} cm/molecule. Uncertainties of $2.0\times10^{-3}\,cm^{-1}$ were adjusted to $1.0\times10^{-3}\,cm^{-1}$.

(2jj) 04MaRoMiNa: A pressure of 17 Torr was used in the whole spectral region; additional recordings at 1 Torr pressure were performed above 6510 cm^{-1} due to the presence of strong lines. As the $HD^{16}O$ absorption lines have been observed in natural abundance, they mostly represent weak lines. Thus, the declared measurement accuracy, better than 0.001 cm^{-1} on average, for these lines was decreased to 0.002 cm^{-1}. Of the 1695 observed transitions, 88.7% (1503 lines) agree with MARVEL transitions with an rms deviation equal to the adopted measurement accuracy of $2\times10^{-3}\,cm^{-1}$. All transitions with measurement accuracy of $3\times10^{-3}\,cm^{-1}$ have been changed to $2\times10^{-3}\,cm^{-1}$.

(2kk) 89OhSa: Absorption spectra of HDO and D_2O recorded using single-mode distributed feedback semiconductor lasers. After recalibration of the experimental spectrum, 96.3% (574 lines) of the 596 observed transitions agree with the MARVEL transitions within an rms deviation of $4.4\times10^{-3}\,cm^{-1}$, as compared to the measurement accuracy of $5.0\times10^{-3}\,cm^{-1}$.

(2ll) 91SaTaIrNa: A near-infrared semiconductor-laser spectrometer was used for measurements of absolute frequencies of 30 vibration–rotation transitions of several molecular species. Three HDO frequencies were measured with an accuracy of about 30 MHz and can be used as a calibration standard in the near infrared region. Vibrational labeling given in the paper was changed by comparison with other assignments: the band studied is not (2 0 1)–(0 0 0) but (0 2 1)–(0 0 0).

(2mm) 05ToTe: Experimental spectra recorded by Schermaul et al. [136] were analyzed here.

(2nn) 01HuHeZhWa: Transitions list supplied by Hu. Of the 899 observed transitions, 85.6% (770 lines) agree with the MARVEL transitions with an rms deviation equal to the declared measurement accuracy of 0.001 cm^{-1}.

(2oo) 05ToNaZoSh: Re-analysis of the absorption spectra of natural abundance water vapor in the 9250–26 000 cm^{-1} region reported previously by Coheur et al. [84] and by Mérienne et al. [88]. The original spectra were recorded by an FTS Bruker IFS 120M coupled with two White multiple-reflection cells of 5 and 50 m base path. The total absorption path was up to 600 m. For weak lines assigned to $HD^{16}O$ absorption, an experimental accuracy of 0.003 cm^{-1} has been adopted in this study, though in the original source the measurement accuracy was declared to be higher (on average). Of the 212 transitions assigned to $HD^{16}O$ absorption, only 58% (212 lines) agree with the MARVEL transitions with an rms deviation equal to the adopted experimental accuracy of 0.003 cm^{-1}, suggesting that the measurement accuracy was indeed slightly overestimated.

(2pp) 00WaHeHuZh: Spectra recorded with the Bruker IFS 120HR FTS of the University of Science and Technology (Hefei, China). Transitions list supplied by Hu. Of the 626 observed transitions, 98.2% (642 lines) agree with the MARVEL transitions with an rms deviation equal to the declared measurement accuracy of 0.003 cm^{-1}. There is an asymmetry in the observed–MARVEL deviations with respect to the zero line: there are 248 positive and 406 negative deviations. A calibration factor for the whole spectral region could not be determined. For 91% of the reported transitions observed–MARVEL deviations are within 0.0016 cm^{-1}, suggesting that the measurement accuracy is better than declared.

(2qq) 03BeNaCa: 55 transitions could not be validated.

(2rr) 08ToTe: A multi-pathlength refit of the data of Schermaul et al. [136,137].

(2ss) 04NaHuHeCa: A 1:1 mixture of H_2O and D_2O was used to make HDO. An additional spectrum of water vapor with much higher concentration of D_2O was recorded. The observed spectrum consists of two parts: 10 110–11 451 and 11 751–12 215 cm^{-1}, containing 1489 and 338 lines, respectively. Of the 1489 observed transitions in the first region, 85.8% (1277 lines) agree with the MARVEL transitions with an rms deviation equal to the declared measurement accuracy of 0.002 cm^{-1}. In the 11 751–12 215 cm^{-1} region there is an asymmetry in the observed–MARVEL deviations with respect to the zero line: there are 252 positive and 84 negative deviations. A calibration factor for this spectral region could not be determined. For 75.4% of the transitions observed–MARVEL deviations are within 0.005 cm^{-1}, suggesting that the experimental accuracy is lower in this region.

(2tt) 08LiHo: CRDS was used for precision measurements of the water line intensities in the 10 603–10 852 cm^{-1} region. Four lines of the $3\nu_3$ band of HDO were measured.

(2uu) 07MaToCa: ICLAS absorption spectra of ^{18}O enriched water were recorded; HDO lines were observed due to high sensitivity of the spectrometer used.

(2vv) 07VoNaCaCo: Assignment of previously reported FTS spectra of Bach et al. [94].

(2ww) 99HuLiHeCh: After applying a calibration factor of 1.00000070 (Table 1), 86% (209 lines) of the 243 observed transitions agree with the MARVEL transitions with an rms deviation equal to the declared measurement accuracy of 0.005 cm^{-1}.

(2xx) 98LaPeSiZh: Absorption spectrum of HDO was investigated using a photo-acoustic spectrometer based on a Ti–Sapphire laser.

(2yy) 01JeMeCaCo: Some of the lines published in this paper were assigned by 07VoNaCaCo [100]. Of the 507 observed transitions, 84.6% (429 lines) agree with MARVEL transitions with an rms deviation equal to the declared measurement accuracy of 0.002 cm^{-1}.

2.9. Comments on the data sources for $HD^{17}O$ given in Table 3

(3a) 78Lovas: 59 microwave transitions reproduced from G. Steenbeckeliers, private communication, July 1971. This data source contains three orphans: 78Lovas.2 at 0.305972, 78Lovas.11 at 0.781876, and 78Lovas.45 at 4.614810 cm^{-1}. 78Lovas.27 is also part of an FSN along with 93Tothb.72.

(3b) 57StTo: The quadrupole hyperfine structure of the $2_{20} \rightarrow 2_{21}$ rotational transition was measured. The unsplit line position is given as 10 374.56 MHz, while the strongest component of the multiplet is estimated as 10 374.31 MHz.

(3c) 93Tothb: 93Tothb.72 is part of an FSN along with 78Lovas.27.

2.10. Comments on the data sources for $HD^{18}O$ given in Table 4

(4a) 78Lovas: 27 microwave transitions reproduced from G. Steenbeckeliers, private communication, July 1971 (seemingly the first observation of the $HD^{18}O$ spectrum). The correct assignment of the pure rotational transition reported at 5902.38 MHz is [4 3 1]←[4 3 2] instead of [4 4 1]←[4 3 2].

(4b) 76FlGi: Commented on in detail in 09MiTaPuSt [114], see its Sections 2 and 6 and Table 4. One of the first studies of water vapor spectra using the Fourier transform technique.

(4c) 06ZeBaKuRi: The line of the [1 1 0]←[1 0 1] transition has been detected at a frequency of 501 567.39 MHz in the atmosphere using the sub-millimeter radiometer (SMR) instrument aboard the Odin satellite.

(4d) 85Johns: Commented on in detail in 09MiTaPuSt [114], see Sections 2 and 6, and Table 4. Note that 24 MW wavenumbers reproduced by Johns from 78Lovas [110] were incorrectly cited in 83MeLuHe [139].

(4e) 06LiDuSoWa: 17 transitions are part of an FSN, seven are ORPs and 13 have been deleted by the MARVEL analysis.

(4f) 93Tothb: See Section 2.2 for comments about recalibration.

(4g) 05Toth: Transitions corresponding to the $2\nu_2$ and ν_1 bands. For more detailed comments see Sections 2 and 6 of 09MiTaPuSt.

(4h) 09MiTaPuSt: Assignment of 38 unassigned lines reported by 07JeDaReTy [101] in the 4205–6588 cm^{-1} range (see Section 3.1 and Table 1 of 09MiTaPuSt) and 970 transitions from 6129 to 10 717 cm^{-1}. The transition (0 2 1)[6 2 4]←(0 0 0)[5 2 3] transition reported at 6538.24339 cm^{-1} is re-assigned to 6538.26139 cm^{-1}.

(4i) 10MiTaDaJe: The transition deleted by MARVEL is: 7015.213870 (0 0 2)[12 1 11]←(0 0 0)[13 1 12], 10MiTaDaJe.186.

(4j) 09LiNaKaCa: This source contains two orphans:

6139.12 (1 0 1)[14 1 13]←(0 0 0)[15 2 14], 09LiNaKaCa.43 and 6139.6 (1 0 1)[14 2 13]←(0 0 0) [15 1 14], 09LiNaKaCa.44. The following transitions have been deleted by the MARVEL analysis:

6157.76 (1 0 1)[13 2 12]←(0 0 0)[14 1 13], 09LiNaKaCa.54 and 6538.88 (1 0 1)[13 2 12]←(0 0 0)[12 1 11], 09LiNaKaCa.945. One transition, 09LiNaKaCa.594 is part of an FSN.

(4k) 07MaToCa: Transitions belonging to the v_2+3v_3 band are commented in 09MiTaPuSt [114], see Sections 2 and 6 and Fig. 4.

3. MARVEL energy levels

Tables 5–7 contain MARVEL vibrational band origins (VBO) for $HD^{16}O$, $HD^{17}O$, and $HD^{18}O$, respectively. The same tables also contain information about the number of rovibrational energy levels validated within this work for each VBO. Observed, MARVEL predicted, and variationally determined spectra of $HD^{16}O$ (VTT [118]), $HD^{17}O$ [116,140], and $HD^{18}O$ [116,140] are reported in

Table 5
MARVEL vibrational band origins (VBO) for $HD^{16}O$, with normal-mode ($v_1v_2v_3$) assignments, MARVEL uncertainties, and the number of validated rotational–vibrational levels (RL) associated with the vibrational levels in the present database.[a]

$v_1v_2v_3$	VBO (cm^{-1})	Unc.[a]	RL
000	0.000000[b]	0	685
010	1403.483724	15	609
100	2723.679737	49	478
020	2782.011177	36	457
001	3707.466740	177	380
110	4099.955912	250	347
030	4145.473186	292	312
011	5089.539837	41	253
200	5363.824480	50	209
040	5420.041442	1016	76
120	5506.186812	250	114
101	6415.460697	42	164
021	6451.899800	75	151
050	6690.413212	999	45
210	6746.908202	36	113
130	[6849.00]		11
002	7250.517890	257	205
031	7754.605467	500	110
111	7808.758612	500	103
060	7914.317012	500	11
300	7918.171912	500	164
220	[8090.15]		16
140	[*8173.13*]		
012	8611.100944	365	151
041	[9032.23]		111
201	9047.068467	500	146
070	[9086.21]		54
121	9155.817812	2499	108
310	9293.001312	536	180
150	9381.786458	497	64
230	9487.915506	491	86
022	9934.772127	873	150
102	9967.016071	1019	152
080	[10 118.42]		6
051	[10 318.47]		12
400	10 378.945940	1224	89
211	10 403.147412	999	19
131	[10 480.59]		2
160	[10 602.72]		1
003	10 631.683126	619	172
320	[10 652.58]		9
240	[*10 789.66*]		
090	[*11 110.69*]		
032	11 242.923202	2499	36
112	11 315.433312	999	54
061	[11 533.36]		10
301	[11 582.72]		86
221	11 701.775912	2499	51
410	11 754.581840	1783	81
170	11 773.312167	2499	7
141	[11 804.55]		11
330	[11 958.60]		27
013	11 969.753013	12	181
250	[12 073.36]		1
0100	[12 164.86]		1
042	[12 516.42]		26
202	12 568.190090	1809	77
122	12 644.652812	2499	57
071	[12 694.33]		3
500	12 767.141475	309	119
180	[12 852.35]		3
311	12 919.938712	2499	78
151	[12 986.79]		9
231	[*13 087.15*]		
023	13 278.350811	46	141
103	13 331.606153	216	126
081	[13 716.47]		1
052	[13 797.38]		5
004	13 853.627343	155	185
212	[*13 889.58*]		
132	[*13 960.04*]		
510	[14 147.42]		31
033	[14 563.09]		8
0120	[14 564.83]		8
113	14 660.721912	315	42
062	[14 997.32]		1
600	15 065.712212	4997	37
302	[15 097.31]		2
014	15 166.104512	17	130
142	15 170.951012	33	30
411	[15 349.50]		2
043	[15 822.14]		1
203	[*15 924.17*]		
1110	[16 047.64]		3
152	[16 449.57]		1
024	16 456.190313	60	75
501	[16 481.72]		3
104	[16 539.04]		42
005	16 920.020712	15	135
114	[17 844.35]		1
063	[18 202.57]		2
015	18 208.446512	48	85
271	[*18 919.13*]		
025	[19 472.44]		25
105	[19 584.53]		21
313	[19 742.09]		1
006	19 836.882808	45	87
701	[*20 952.89*]		
106	22 454.468792	500	40
007	22 625.523004	2161	51
116	[*23 700.84*]		

[a] The uncertainties (Unc.) are given in units of $10^{-6}\,cm^{-1}$. For VBOs not determined by the available experimental data, approximate variationally computed VBOs, based on an exact kinetic energy operator and the PES of Yurchenko et al. [119], are given in brackets. These values should only be used for guidance about the VBOs, although their accuracy is expected to be better than $0.1\,cm^{-1}$. No uncertainties are given for these VBOs. For completeness, VBOs for which no rovibrational states have been observed are also given. These levels, for which no RL values are given, are printed in italics and correspond to variationally computed values, as well. The VBOs are ordered according to energy.

[b] The value of the vibrational ground state was fixed to zero with zero uncertainty.

Table 6
MARVEL vibrational band origins (VBO) for $HD^{17}O$, with normal-mode ($v_1v_2v_3$) assignments, MARVEL uncertainties, and the number of rotational levels (RL) the vibrational levels are holding within the present database.[a]

$v_1v_2v_3$	VBO (cm^{-1})	Unc.	RL
0 0 0	0.000000[b]	0	86
0 1 0	1399.674626	182	76

[a] See footnote a to Table 5.
[b] See footnote b to Table 5.

Table 7
MARVEL and RITZ vibrational band origins (VBO) for $HD^{18}O$, with normal-mode ($v_1v_2v_3$) assignments, uncertainties, and the number of rotational levels (RL) the vibrational levels are holding within the related databases.[a]

$v_1v_2v_3$	MARVEL			RITZ [114]	
	VBO (cm^{-1})	Unc.	RL	VBO/cm^{-1}	Unc.
0 0 0	0.000000[b]	0	168	0.000000[b]	0
0 1 0	1396.266365	176	155	1396.266540	299
1 0 0	2709.284316	178	125	2709.284528	311
0 2 0	2767.209640	220	84	2767.212120	696
0 0 1	3696.330134	345	153	3696.330305	696
1 1 0	4080.544716	484	99	4080.544949	484
0 3 0	4121.754251	349	75	4121.754430	348
0 1 1	5071.496323	352	115	5071.496500	696
0 4 0			7		
2 0 0	5335.360667	485	71	5335.360899	484
1 0 1	6390.982474	189	133	6390.982322	188
0 2 1	6425.951205	175	109	6425.951439	342
2 1 0	6711.672686	173	80	6711.672989	185
0 0 2	7229.185072	227	135	7229.185309	226
0 5 0			11		
0 3 1			10		
1 1 1			11		
1 2 1			1		
3 0 0	7876.171252	399	47	7876.171489	676
0 2 2			23		
1 0 2	9930.723962	968	29	9930.724199	966
0 1 2			79		
2 0 1			3		
0 0 3			61		
0 7 0			1		
3 1 0			5		
0 1 3			69		
4 0 0			4		
3 0 1			1		

[a] See footnote a to Table 5.
[b] See footnote b to Table 5.

Figs. 4–6, respectively. As in Part I, the MARVEL energy levels were graded as A^+, A^-, B^+, B^-, and C, given in the Supplementary Material.

3.1. $HD^{16}O$

For $HD^{16}O$, 53 291 transitions of the 54 740 initial transitions have been validated and used in the final MARVEL analysis. From these transitions we derive a final set of 8818 energy levels which belong to 54 vibrational states and have J up to 30 and K_a up to 21. 66 transitions from 03JaTeBeZo [86] form an FSN and 13 transitions from the same source are orphans; thus, they could not be used for energy level determination.

A comparison of the experimental (MARVEL) and variational (VTT [118]) energy level values is given in Fig. 2. The root-mean-square deviation for this comparison is 0.058 cm^{-1}, with the maximum obs–calc residuals being -0.51 and -1.27 cm^{-1} for the [4 0 4] and [3 0 3] levels of the (0 6 3) vibrational state, respectively. The (0 6 3) [3 0 3] energy level at 18 293.1607 cm^{-1} was derived from two weak lines in 07VoNaCaCo [100] and should most likely be considered incorrect. Note that these two levels were excluded when the above quoted rms deviation was determined.

A comparison can be made between the original set of observed transitions and those calculated from the experimental energy levels determined by MARVEL; this is presented in Fig. 3. The differences do not exceed 0.038 cm^{-1}; 52.6% and 84% of all transitions are reproduced within 0.001 and 0.005 cm^{-1}, respectively. Only 5.6% of the observed transitions differ from the MARVEL calculated values by more than 0.01 cm^{-1}.

MARVEL may increase, via robust reweighting, an experimental uncertainty of a transition when it is not consistent with that derived from the MARVEL energy levels. For transitions with low J and K_a values it is rather easy to evaluate a feasible experimental uncertainty if enough CDs are available. However, for increased values of J and K_a the CD relations become less accurate and instructive, a number of experimental lines represent unresolved multiplets, and it becomes more and more difficult to judge properly the actual experimental accuracy of the transitions. This in turn limits the accuracy of the MARVEL energy levels derived. This situation could be improved only by including additional accurate experimental information in the MARVEL input file.

The set of MARVEL energy levels derived from processing the validated observed transitions has been used to predict a large number of rovibrational transitions with positions at the level of experimental accuracy. These line positions were augmented with variational intensities. The total number of predicted transitions with intensities larger than 1.0×10^{-29} cm molecule^{-1} is 188 565 for T = 296 K. Observed, observed + predicted, and variational transitions are shown in Fig. 4 for $HD^{16}O$. The number of residual unobserved variational lines was obtained as the difference between the variationally calculated and observed + predicted transitions; their number is 185 751 with intensities greater than 1×10^{-29} cm molecule^{-1}. This figure is especially important for future experimental studies of the high-resolution spectra of $HD^{16}O$. The strongest unobserved lines fall in the 3600–9600 and 9600–12 400 cm^{-1} regions with intensities 3×10^{-23} and 4×10^{-25} cm molecule^{-1}, respectively. Interestingly, in the spectral region below 2400 cm^{-1} intensities of the residual lines do not exceed 1×10^{-27} cm molecule^{-1}, and in the 2400–3600 cm^{-1} region their intensities are not larger than 1×10^{-26} cm molecule^{-1}. Such a complete coverage of the 0–2400 cm^{-1} region by the obs +

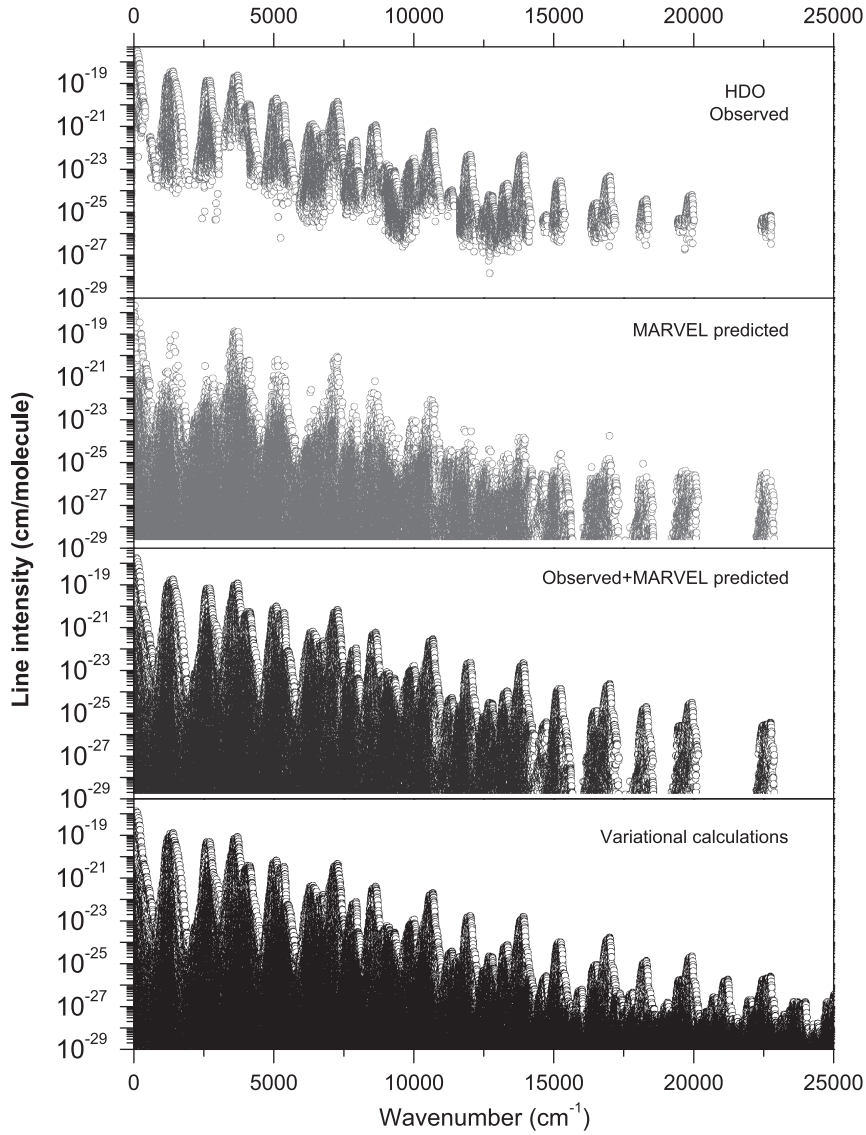

Fig. 4. Observed (top panel), MARVEL predicted (second panel), their sum (third panel) transitions based on predictions from the VTT variational calculations [118] (bottom panel) for $HD^{16}O$. Calculated line intensities are used in each case.

predicted transitions is due to energy levels derived from the analysis of hot spectra in 03JaTeBeZo [86]. Similarly to the "cold" spectrum, a set of 74 122 "hot" transitions at T = 1770 K in the 380–3932 cm^{-1} region have been predicted at a level of experimental accuracy in positions using MARVEL energy levels and variational intensities larger than 1.0×10^{-24} cm molecule^{-1}.

We considered three sources of hot $HD^{16}O$ transitions, Refs. [64,82,86]. The list given in 03JaTeBeZo [86] includes the transitions given by 01PaBeZoSh [82], so it was not necessary to analyze the second source independently. Since hot water spectra have been measured for the most abundant isotopologue, $HD^{16}O$, the largest J is high, J_{max} = 30. Then, one can observe that, due to the large number of measured transitions, the list of VBOs is fairly complete for $HD^{16}O$ and there are very few VBOs below 15 000 cm^{-1} for which rotational–vibrational levels have not been determined. In fact, the only lower-lying VBOs which are missing are (1 4 0), (2 4 0), (0 9 0), (2 3 1), (1 3 2), and (2 1 2). At higher wavenumbers a high proportion of VBOs still appear (Table 5). The highest states for which VBOs and rovibrational levels have been measured contain seven quanta of stretch: 51 and 40 rotational levels have been determined for the (0 0 7) and (1 0 6) VBOs, respectively. We note that double resonance measurements [97] give data on VBOs higher than these; however, this work presents no measured transition wavenumbers and we were therefore unable to use it in this study.

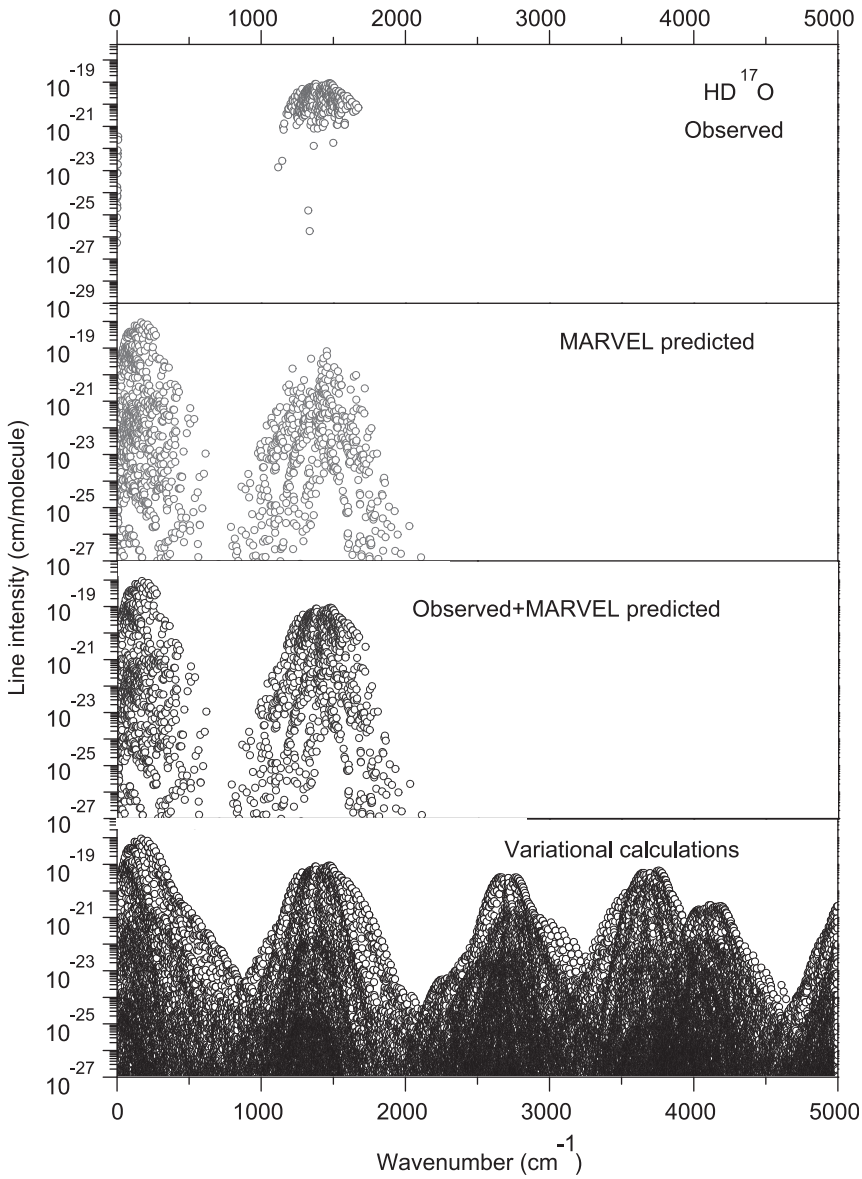

Fig. 5. Observed (top panel), MARVEL predicted (second panel), their sum (third panel) transitions based on predictions from variational calculations [116,140] (bottom panel) for $HD^{17}O$. Calculated line intensities are used in each case.

3.2. $HD^{17}O$ and $HD^{18}O$

Of the 485 transitions in the MARVEL database of $HD^{17}O$, 478 were validated and these led to 162 MARVEL energy levels with a maximum J value of 11. There is only one VBO determined for $HD^{17}O$, (0 1 0) (Table 6 and Fig. 5). As is clear from Fig. 5, the energy levels determined for this band allow one to make excellent predictions of a large number of pure rotational levels on the ground vibrational state (0 0 0). Future experimental investigations should validate these MARVEL predictions.

As to $HD^{18}O$, of the 8729 transitions in the MARVEL database, 8634 were validated and these led to the determination of 1860 MARVEL energy levels with a maximum J value of 18. Several recent studies have addressed the assignment of the high-resolution rovibrational spectrum of $HD^{18}O$, including 06LiDuSoWa [138], 09MiTaPuSt [114], 09LiNaKaCa [108], and 10MiTaDaJe [115]. While there have been a relatively small number of assigned transitions for $HD^{18}O$ before, 06LiDuSoWa changed this situation drastically. Furthermore, the experimental database of $HD^{18}O$ was treated by the code RITZ in 09MiTaPuSt [114] and 10MiTaDaJe [115]. The RITZ code is similar to MARVEL and results in energy levels and their uncertainties. Table 7 compares the MARVEL and the RITZ VBO and uncertainty values. The recommended values remain those obtained using the present database and the MARVEL protocol.

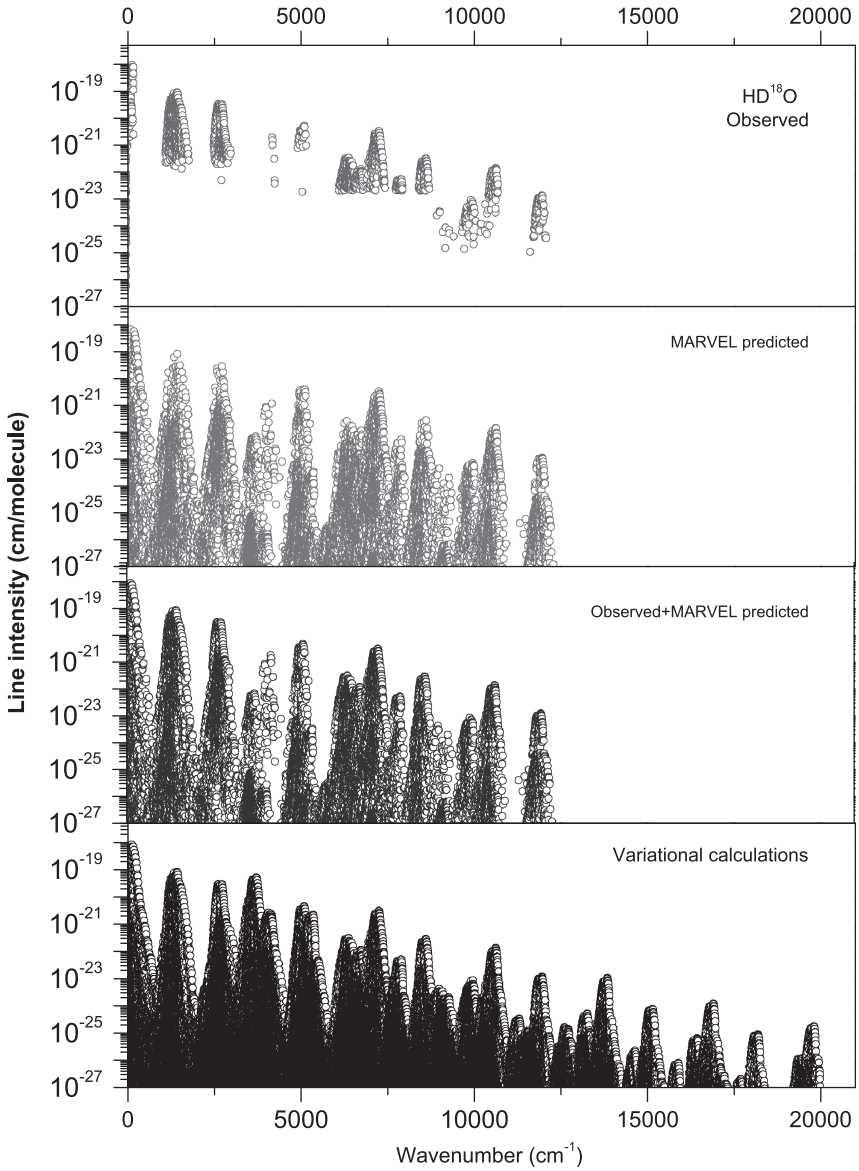

Fig. 6. Observed (top panel), MARVEL predicted (second panel), their sum (third panel) transitions based on predictions from variational calculations [116,140] (bottom panel) for $HD^{18}O$. Calculated line intensities are used in each case.

3.3. Status of highly accurate transitions

The agreement between the MARVEL predicted and the experimental pure rotational transitions improved slightly by the recalibration of the experimental transitions. Nevertheless, the MARVEL uncertainties of the pure rotational levels is still uniformly larger than is usual for lines coming from microwave determinations. To show that this is due to the uncertainties of the upper states we performed a MARVEL analysis of the pure rotational states. MARVEL can reproduce the microwave uncertainties very nicely, down to the level of the experimental uncertainties, as also observed before [5]. For example, the mean of the reproduction of the pure rotational lines for $HD^{16}O$ is $2.3\times10^{-5}\,cm^{-1}$ if only the (0 0 0) transitions are employed in the MARVEL analysis. The agreement worsens to $4.8\times10^{-5}\,cm^{-1}$ if the full calibrated database is used to predict the pure rotational transitions.

Another source of inaccuracy when combining measured results from several sources is due to pressure shifts. This is especially of concern for this study as the pressure of HDO had to be increased several times in order to allow the detection of the HDO lines. Since there is no theory of pressure shifts of sufficient accuracy, no attempt was made in this work to correct the observed lines to, for example, zero pressure. This introduces a perhaps appreciable uncertainty for most of the measured lines. This is reflected in MARVEL uncertainties larger than

otherwise expected for many rotational–vibrational levels.

Of all the transitions outside of the micro- and millimeterwave regions treated in this study, the most accurate one available is at 1480.094038033(67) cm^{-1} [76], observed for $HD^{16}O$. Toth [72] has measured the same transition although with much less precision. Guelachvili [47] also measured this transition (as expected, his measured value only agrees with the other ones after the multiplicative recalibration of his results). As the present study of all the measured transitions of $HD^{16}O$ shows, the lower (0 0 0) 5_{15} and the upper (0 1 0) 5_{24} energy levels of this transition are involved in 461 and 76 transitions, respectively. This means that MARVEL can fix the energies of these levels, and thus the transition, with considerable certainty. The MARVEL wave number and uncertainty of this transition is 1480.094038033(7000) cm^{-1}. Therefore, it is clear that MARVEL (a) did not change the value of the transition known accurately and precisely, and (b) increased the uncertainty of the measured line considerably. None of this is surprising given the large number of much less precisely determined transitions the two energy levels are involved in and the fact that MARVEL did not find it necessary to adjust the uncertainty of the original experimental measurement (which confirms its high precision).

4. Discussion

4.1. A comparison with HITRAN

The relevant features of the HITRAN database [141,142] are summarized in the original publications and in Part I; thus, they are not repeated here in detail, and just a few remarks are made. Table 8 compares the data used in this study with those in the HITRAN [141] database. There are several notable differences between HITRAN and the (present) IUPAC water-vapor data analysis. First, HITRAN contains a mixture of observed and calculated entries, whereas the lines used in the present analysis are based strictly on published experimental values. Even though the goal in HITRAN is to have a complete set of self-consistent and maintainable values, in practice this is not possible at this time. Entries that have been determined under controlled laboratory conditions and are very accurate are frequently used in HITRAN. However, in order to have adequate sets of lines for important vibration–rotation bands, it is necessary to use theoretical extrapolations of the data (especially to the higher rotational levels), to have calculations of lines that are blended or obscured in laboratory observations, or to have calculations for quantities that theory actually yields better constrained values at present than experiment (some line-shape parameters, for example). Second, in the case of multiple sets of data for a quantity, HITRAN takes each datum from a single source. This consolidation of data has been made by judgment of the quality of the different data sets. With the superior structure of the IUPAC database, all high-quality data have been retained. In principle one can use a filtering code to produce a smaller list for a specific application. Third, HITRAN is aimed at atmospheric temperature applications and, by application of a minimum transition intensity at 296 K requirement, rejects many hot transitions; our present analysis aims to capture all measured transitions. The increased number of transitions in the present compilation is partly a reflection of this.

Table 8
Comparison of $HD^{16}O$, $HD^{17}O$, and $HD^{18}O$ transition data found in HITRAN [141] and used in the present compilation.

	$HD^{16}O$	$HD^{17}O$	$HD^{18}O$
Total number of transitions in present database	54 740	485	8728
Unique transitions in present database	36 690	445	7186
Number of validated transitions	53 291	478	8635
Transitions in HITRAN database	13 238	175	1611
Concordant transitions[a]	9627	169	848
Transitions absent in present database	3611	6	763
Transitions absent in HITRAN	27 063	276	6338

[a] Transitions which are present both in HITRAN and in the present validated IUPAC database.

The line positions of $HD^{16}O$ in the pure rotational band have remained unchanged in HITRAN since the 1986 edition [132] and originate from an older version of the JPL catalog [143]. It was generated based on the constants obtained in the simultaneous fit of submillimeter measurements of Messer et al. [49] and a set of experimentally determined ground state energy levels based on infrared measurements in the v_2 band. All the lines from 500 to 7514 cm^{-1} originate from the SISAM database [144]. Most of the $HD^{16}O$ lines in SISAM are experimentally observed, while 1525 were calculated based on the experimentally determined energy levels. There are no $HD^{16}O$ lines between 7514 and 9751 cm^{-1}. From 9751 to 10 782 cm^{-1}, data from Tolchenov and Tennyson [107] were used, and starting from 11 750 cm^{-1} lines were taken from Voronin et al. [100].

For $HD^{18}O$, the current version of the JPL catalogue [145] was used in HITRAN for the pure rotational band and data from Toth's website [144] was used for all other lines from 500 to 3825 cm^{-1}. Note that line positions of 56 of these lines were determined from experimentally derived energy levels rather than directly measured. The majority of 6338 lines in the IUPAC dataset of experimental transitions that are absent in HITRAN (see Table 8) are lines above 3825 cm^{-1}.

For $HD^{17}O$, the only lines in HITRAN are those from the SISAM database [144], while IUPAC data include measurements in the pure rotational band [111,110] and the v_2 band from 93Tothb [61].

4.2. Completeness of data

As shown in Part I, a comparison between the variational nuclear motion calculations and the results of the MARVEL analysis can be used to assess the overall completeness of the spectroscopic data for each water

isotopologue and to indicate key regions for further experimental study. In this context the results of the MARVEL analysis can be used to predict new transitions between already determined energy levels but cannot be extrapolated to transitions involving unobserved energy levels.

Figs. 4, 5, and 6 show comparisons of numbers of room temperature transitions for $HD^{16}O$, $HD^{17}O$, and $HD^{18}O$, respectively. Each figure gives the measured transitions, the number of new transitions predicted from the MARVEL energy levels, the sum of these and the transitions predicted by the variational calculations. For simplicity the VTT [118] calculated transition intensities are assumed throughout.

One interesting measure of completeness is the proportion of the integrated absorption recovered for each isotopologue, a summary of which is given in Table 9. For $HD^{16}O$, the measurements recover 86% of the total absorbance at 296 K. The extra transitions involving energy levels predicted by MARVEL yield 14% of the total absorbance meaning that the combined transitions lead to essentially total recovery of the absorbance. This result is significant because, given that the *ab initio* calculated transition intensities have been proven to be reliable [146,147], it means very reliable estimates of missing absorption can be generated using very precise estimates of the frequencies. We note that at higher temperatures we expect the percentage of the total absorbance recovered experimentally to drop.

Unsurprisingly, the proportion of data observed for the minor isotopologues is less than for $HD^{16}O$. Under these circumstances the use of MARVEL alone cannot provide all the missing absorption. However, improvement in the simulation of the bands where only partial data is available is still significant.

5. Conclusions

Among many other applications of such data, a huge quantity of high-quality molecular data are needed for the understanding of spectroscopic measurements related to different stars and the atmospheres of planets and exoplanets. One must know precise positions and usually intensities and line shapes in order to be able to judge what is observed and how much of that species is present. Among the species for which spectroscopic data are needed for this or other important scientific or engineering applications, water is probably the single most important one. Thus, the study of the complete spectra of its isotopologues is of prime importance. At the same time, the high-resolution rovibrational spectra of the isotopologues of the water molecule form a fertile testing ground for different experimental and theoretical approaches yielding the required information.

While the ambitious aim of the IUPAC Task Group partially responsible for this work is to create a complete linelist for all isotopologues of water, a first step is to determine energy levels and line positions. This paper provides, for the first time, a dependable and carefully validated set of energy levels and transition wavenumbers, all with dependable and self-consistent uncertainties, for $HD^{16}O$, $HD^{17}O$, and $HD^{18}O$. As demonstrated in this work, the MARVEL approach [3–5], combined with results from variational nuclear motion computations, provides an ideal platform to achieve this goal.

Our analysis of the available HDO line frequency measurements pointed towards some issues with calibration of the published data. We were not always able to resolve these issues and it is our view that an effort to develop modern frequency standards, such as that of Guelachvili et al. [130], is urgently needed.

The distributed information system W@DIS [148,149], containing the transitions and the energy levels of this study, can be accessed via http://wadis.saga.iao.ru.

Acknowledgements

We all thank the International Union of Pure and Applied Chemistry for funding under project 2004-035-1-100 (A database of water transitions from experiment and theory). In addition, this work has received partial support from the UK Natural Environment Research Council, the Royal Society, Grant WWLC-008535-(reintegration) MCA FP6 EC, the Scientific Research Fund of Hungary (Grant OTKA K77825), the European Union QUASAAR Marie Curie research training network, NATO, the Russian Foundation for Basic Research, the Belgian Federal Science Policy Office (contracts EV/35/3A, SD/AT/01A, PRODEX 1514901NLSFe(IC)), the Belgian National Fund for Scientific Research (FRFC contracts), the Communauté de Belgique (Action de Recherche Concertées), the NASA laboratory astrophysics program, NASA Earth Observing System (EOS), under Grant NNX08AD92G, the National Science Foundation, through Grant no. ATM-0803135, and the Programme National LEFE (CHAT) of CNRS (INSU). Part of the research described in this paper was performed at

Table 9
Proportion of the total integrated absorption[a] at 296 K, as estimated using the VTT [118] variational line list ("calc"), of the three isotopologues of HDO recovered experimentally ("expt") and by including the extra transitions predicted by the MARVEL protocol ("MARVEL"). Note that different wavenumber maximum (ν_{max} in cm^{-1}) and intensity cut-offs have been used for each isotopologue; these choices were dictated by the available experimental data.

	ν_{max}	Cut-off	A(calc)	A(expt)	$\frac{A(expt)}{A(calc)}$ (%)	A(MARVEL)	$\frac{A(expt)+A(MARVEL)}{A(calc)}$ (%)
$HD^{16}O$	25 000	10(−29)	5.95(−17)	5.13(−17)	86	8.66(−18)	100
$HD^{17}O$	5000	10(−28)	5.74(−17)	9.22(−18)	16	3.43(−17)	66
$HD^{18}O$	20 000	10(−27)	5.79(−17)	3.50(−17)	60	1.60(−17)	88

[a] Absorption (A) and intensities in cm molecule^{-1}; powers of 10 given in parenthesis.

Table 10
Data sources additional to those presented in Part I and their characteristics for $H_2{}^{17}O$.[a]

Tag	Range (cm^{-1})	Trans. A/V	Physical conditions					Comments
			T (K)	p (hPa)	Abun. (%)	Rec.	L (m)	
86GuRa [150]	100–1986	203/202						(10a)
09LiNaKaCa [108]	5907–6726	212/212	299	0.13–13	0.3	CRDS		(10b)

[a] See footnote a to Table 2.
(10a) 86GuRa. MARVEL cuts the transition 83GuRa.5 at 207.73575 cm^{-1}.
(10b) 09LiNaKaCa. $H_2{}^{17}O$ transitions assigned in the CRDS spectrum of a highly ^{18}O enriched sample.

the Jet Propulsion Laboratory, California Institute of Technology, under contract with the National Aeronautics and Space Administration.

Appendix A

The MARVEL protocol involves active maintenance (the A in MARVEL) and periodic update of the databases containing the measured transitions. Since the publication of Part I [1], new measurements [108,150] came to our attention for $H_2{}^{17}O$ and $H_2{}^{18}O$, the two water isotopologues treated there. Furthermore, during preparation of the Part II manuscript the MARVEL procedure, as noted above, has also been slightly adjusted in order to determine more reliable energy values and uncertainty estimates via a post-MARVEL validation scheme. Therefore, in this appendix we give improved VBOs for $H_2{}^{17}O$ and $H_2{}^{18}O$ and in the Supplementary Material we provide new or improved MARVEL energy levels for these two isotopologues, as well. These new data should replace the ones presented in Part I.

A.1. $H_2{}^{17}O$

Two new sources have been added to the Part I database, 09LiNaKaCa [108] and 86GuRa [150]. Characteristics of these two sources are given in Table 10. Compared to Part I, the number of validated transitions increased from 8614 to 9028 and the number of energy levels increased from 2687 to 2723.

Application of the post-MARVEL validation scheme also meant that the MARVEL energy levels for this isotopologue changed as compared to Part I. The full set of VBOs and their improved uncertainties are given in Table 11. There are no new VBOs compared to Part I. The improved set of MARVEL rotational–vibrational energy levels are provided in the Supplementary Material.

Table 11
MARVEL vibrational band origins (VBO), with polyad quantum number ($P=2v_1+v_2+2v_3$), normal-mode ($v_1v_2v_3$) and local-mode ($(mn)^{\pm}v_2$) assignments, MARVEL uncertainties (Unc.), and the number of rotational levels (RL) the vibrational levels are holding within the present, improved database, for $H_2{}^{17}O$.[a]

P	$v_1v_2v_3$	$(mn)^{\pm}v_2$	VBO (cm^{-1})	Unc.	RL
0	000	$(00)^{+}0$	0.000000[b]	0	192
1	010	$(00)^{+}1$	1591.325719	47	153
2	020	$(00)^{+}2$	3144.980520	46	78
2	100	$(10)^{+}0$	3653.142275	28	108
2	001	$(10)^{-}0$	3748.318105	31	141
3	110	$(10)^{+}1$	5227.705615	473	69
3	011	$(10)^{-}1$	5320.251393	527	157
4	120	$(10)^{+}2$	6764.725615	473	73
4	021	$(10)^{-}2$	6857.272485	47	94
4	200	$(20)^{+}0$	7193.246415	47	81
4	101	$(20)^{-}0$	7238.714012	51	110
4	002	$(11)^{+}0$	7431.076115	473	27
5	111	$(20)^{-}1$	8792.544010	360	108
5	012	$(11)^{+}1$	8982.869215	473	55
6	121	$(20)^{-}2$	10311.201787	440	75
6	201	$(30)^{-}0$	10598.475620	492	103
6	102	$(21)^{+}0$	10853.505315	473	69
6	003	$(21)^{-}0$	11011.882910	2465	84
7	131	$(20)^{-}3$	11792.822200	490	40
7	211	$(30)^{-}1$	12132.992610	493	94
7	013	$(21)^{-}1$	12541.227060	517	51
8	221	$(30)^{-}2$	13631.499810	542	52
9	071	$(10)^{-}7$	13808.273310	493	2
8	301	$(40)^{-}0$	13812.158110	493	74
8	103	$(31)^{-}0$	14296.279510	197	36
10	321	$(40)^{-}2$	16797.167510	3944	70
10	401	$(50)^{-}0$	16875.620510	3944	55

[a] The uncertainties (Unc.) are given in units of 10^{-6} cm^{-1}. The VBOs are ordered by energy.
[b] The value of the vibrational ground state was fixed to zero with zero uncertainty.

A.2. $H_2{}^{18}O$

Three new sources have been added to the Part I database, 09LiNaKaCa [108], 09PuCaHaVa [151], and 86GuRa [150]. Characteristics of these sources are given in Table 12. There are six orphans in the database and an FSN containing 22 transitions. Compared to Part I, the number of validated transitions increased from 29 364 to 31 705 and the number of energy levels increased from 4849 to 5131.

Application of the post-MARVEL validation scheme also meant that the MARVEL energy levels for $H_2{}^{18}O$ isotopologue changed as compared to Part I. The full set of VBOs and their improved uncertainties are given in Table 13. The improved set of MARVEL energy levels are provided in the Supplementary Material.

Table 12
Data sources additional to those presented in Part I and their characteristics for $H_2{}^{18}O$.[a]

Tag	Range (cm^{-1})	Trans. A/V	Physical conditions					Comments
			T (K)	p (hPa)	Abun. (%)	Rec.	L (m)	
09PuCaHaVa [151]	6.4–18.4	5/5	RT					
86GuRa [150]	55–2053	351/350						(12a)
09LiNaKaCa [108]	5907–6726	2015/2006	299	0.13–13	84–92	CRDS		

[a] See footnote a to Table 2:
(12a) 86GuRa. MARVEL cuts the transition 83GuRa.21 at 147.19380 cm^{-1}.

Table 13
MARVEL vibrational band origins (VBO), with polyad quantum number ($P=2v_1+v_2+2v_3$), normal-mode ($v_1v_2v_3$) and local-mode ($(mn)^{\pm}v_2$) assignments, MARVEL uncertainties, and the number of rotational levels (RL) the vibrational levels are holding within the present revised database, for $H_2{}^{18}O$.[a]

P	$v_1v_2v_3$	$(mn)^{\pm}v_2$	VBO (cm^{-1})	Unc.	RL
0	000	$(00)^{+}0$	0.000000	0	298
1	010	$(00)^{+}1$	1588.276029	22	227
2	020	$(00)^{+}2$	3139.050028	36	146
2	100	$(10)^{+}0$	3649.685417	50	192
2	001	$(10)^{-}0$	3741.566775	45	216
3	030	$(00)^{+}3$	4648.477809	341	130
3	110	$(10)^{+}1$	5221.243308	377	170
3	011	$(10)^{-}1$	5310.461383	281	246
4	120	$(10)^{+}2$	6755.510366	283	167
4	021	$(10)^{-}2$	6844.598785	194	169
4	200	$(20)^{+}0$	7185.878096	506	176
4	101	$(20)^{-}0$	7228.883501	493	181
4	002	$(11)^{+}0$	7418.724061	294	147
5	130	$(10)^{+}3$	8249.037152	459	79
5	031	$(10)^{-}3$	8341.107933	417	120
5	210	$(20)^{+}1$	8739.525858	503	84
5	111	$(20)^{-}1$	8779.719569	349	143
5	012	$(11)^{+}1$	8967.565058	503	87
6	041	$(10)^{-}4$	9795.331502	473	72
6	220	$(20)^{+}2$	10256.584858	503	61
6	121	$(20)^{-}2$	10295.634509	450	108
6	022	$(11)^{+}2$	10483.221458	503	53
6	300	$(30)^{+}0$	10573.916858	503	97
6	201	$(30)^{-}0$	10585.285174	460	133
6	102	$(21)^{+}0$	10839.955723	499	90
6	003	$(21)^{-}0$	10993.681009	450	103
7	230	$(20)^{+}3$	11734.525057	503	68
7	131	$(20)^{-}3$	11774.707602	373	103
7	032	$(11)^{+}3$	11963.537158	503	73
7	310	$(30)^{+}1$	12106.977658	503	98
7	211	$(30)^{-}1$	12116.797008	466	133
7	112	$(21)^{+}1$	12372.705608	410	103
7	013	$(21)^{-}1$	12520.122915	47	110
8	221	$(30)^{-}2$	13612.710202	47	74
8	301	$(40)^{-}0$	13795.398204	47	94
8	202	$(31)^{+}0$	14187.982458	1358	49
8	103	$(31)^{-}0$	14276.336099	464	68
10	321	$(40)^{-}2$	16775.380902	1418	28
10	401	$(50)^{-}0$	16854.990902	1418	44

[a] See footnotes a and b to Table 11.

Appendix B. Supplementary data

Supplementary data associated with this article can be found in the online version at doi:10.1016/j.jqsrt.2010.06.012.

References

[1] Tennyson J, Bernath PF, Brown LR, Campargue A, Carleer MR, Császár AG, et al. Critical evaluation of the rotational-vibrational spectra of water vapor. Part I. Energy levels and transition wavenumbers for $H_2{}^{17}O$ and $H_2{}^{18}O$. J Quant Spectrosc Radiat Transfer 2009;110:573–96.
[2] Bernath PF. The spectroscopy of water vapour: experiment, theory and applications. Phys Chem Chem Phys 2002;4:1501–9.
[3] Császár AG, Czakó G, Furtenbacher T, Mátyus E. An active database approach to complete spectra of small molecules. Ann Rep Comp Chem 2007;3:155–76.
[4] Furtenbacher T, Császár A, Tennyson J. MARVEL: measured active rotational–vibrational energy levels. J Mol Spectrosc 2007;245:115–25.
[5] Furtenbacher T, Császár AG. On employing $H_2{}^{16}O$, $H_2{}^{17}O$, $H_2{}^{18}O$, and $D_2{}^{16}O$ lines as frequency standards in the 15–170 cm^{-1} window. J Quant Spectrosc Radiat Transfer 2008;109:1234–51.
[6] Joussaume S, Sadourny R, Jouzel J. A general circulation model of water isotope cycles in the atmosphere. Nature 1984;311:24–9.
[7] Fouchet T, Lellouch E. Vapor pressure isotope fractionation effects in planetary atmospheres: application to deuterium. Icarus 2000;144:114–23.
[8] Montmessin F, Fouchet T, Forget F. Modeling the annual cycle of HDO in the Martian atmosphere. J Geophys Res 2005;110:E03006.
[9] Payne VN, Noone D, Dudhia A, Piccolo C, Grainger RG. Global satellite measurements of HDO and implications for understanding the transport of water vapour into the stratosphere. J Quart Roy Meteor Soc 2007;133:1459–71.
[10] Steinwagner J, Milz M, von Clarmann T, Glatthor N, Grabowski U, Höpfner M, et al. HDO measurements with MIPAS. Atmos Chem Phys 2007;7:2601–15.
[11] De Bergh C, Bezard B, Owen T, Crisp D, Maillard J-P, Lutz BL. Deuterium on Venus—observations from Earth. Science 1991;251:547–9.
[12] Pavlenko YV, Harris GJ, Tennyson J, Jones HRA, Brown JM, Harrison J, et al. The electronic bands of CrD, CrH, MgD and MgH: application to the "deuterium" test. Mon Not R Astr Soc 2008;386:1338–46.
[13] Hewitt AJ, Doss N, Zobov NF, Polyansky OL, Tennyson J. Deuterated water: partition functions and equilibrium constant. Mon Not R Astr Soc 2005;356:1123–6.
[14] Watson JKG. Robust weighting in least-squares fits. J Mol Spectrosc 2003;219:326–8.
[15] Townes CH, Merrit FR. Water spectrum near one-centimeter wavelength. Phys Rev 1946;70:558–9.
[16] Strandberg MWP, Wentink Jr T, Hillger RE, Wannier GH, Deutsch ML. Stark spectrum of HDO. Phys Rev 1948;73:188.
[17] McAfee Jr KB. A study of the absorption of some gases at microwave frequencies. PhD thesis, Harvard; 1949 [data given by [22]].
[18] Strandberg MWP. Rotational absorption spectrum of HDO. J Chem Phys 1949;17:901–4.
[19] Jen CK. Rotational magnetic moments for H_2O and HDO. Phys Rev 1949;76:471.
[20] Jen CK. Rotational magnetic moment in polyatomic molecules. Phys Rev 1951;81:197–203.
[21] Beerd Y, Weisbaum S. An ultra-high frequency rotational line of HDO. Phys Rev 1953;91:1010–4.
[22] Jen CK, Bianco DR, Massey JT. Some heavy water rotational absorption lines. J Chem Phys 1953;21:520–5.
[23] Burke BF, Strandberg MWP. Zeeman effect in rotational spectra of asymmetric-rotor molecules. Phys Rev 1953;90:303–8.

[24] Crawford HD. Two new lines in the microwave spectrum of heavy water. J Chem Phys 1953;21:2099.
[25] Posener DW, Strandberg MWP. Microwave spectrum of HDO. J Chem Phys 1953;21:1401–2.
[26] Posener DW, Strandberg MWP. Centrifugal distortion effect in asymmetric top molecules III. H_2O, D_2O, and HDO. Phys Rev 1954;95:374–84.
[27] Weisbaum S, Beers Y, Hermann G. Low-frequency rotational spectrum of HDO. J Chem Phys 1955;23:1601–5.
[28] Erlandson G, Cox J. Millimeter-wave lines of heavy water. J Chem Phys 1956;25:778–9.
[29] Benedict WS, Gailar N, Plyler EK. Rotation–vibration spectra of deuterated water vapor. J Chem Phys 1956;24:1139–65.
[30] Posener DW. Hyperfine structure in the microwave spectrum of water. Austr J Phys 1957;10:276–85.
[31] Gailar NM, Dickey FP. The vibration–rotation band v_2 of HDO vapor. J Mol Spectrosc 1960;4:1–15.
[32] Treacy EB, Beers Y. Hyperfine structure of the rotational spectrum of HDO. J Chem Phys 1962;36:1473–80.
[33] Thaddeus P, Krisher LC, Loubser JHN. Hyperfine structure of the microwave spectrum of HDO, HDS, CH_2O, and CHDO: beam-maser spectroscopy and asymmetric-top molecules. J Chem Phys 1964;40:257–73.
[34] Bluyssen H, Verhoeven J, Dymanus A. Hyperfine structure of HDO and D_2O by beam maser spectroscopy. Phys Lett A 1967;25:214–5.
[35] Verhoeven J, Bluyssen H, Dymanus A. Hyperfine structure of HDO and D_2O by beam maser spectroscopy. Phys Lett A 1968;26:424–5.
[36] Steenbeckeliers G, Bellet J. Spectre de rotation de l'eau lourde. C R Hebd Seances Acad Sci B 1970;270:1039–41.
[37] Bellet J, Steenbeckeliers G. Calcul des constantes rotationnelles des molecules H_2O, HDO et D_2O dans leurs etats fondamentaux de vibration. C R Hebd Seances Acad Sci B 1970;271:1208–11.
[38] De Lucia FC, Cook RL, Helminger P, Gordy W. Millimeter and submillimeter wave rotational spectrum and centrifugal distortion effects of HDO. J Chem Phys 1971;55:5334–9.
[39] Lafferty W, Bellet J, Steenbeckeliers G. Spectre microonde des transitions de faible intensité de la molécule HDO. Etude de la molecule dans l'état vibrationell exité v_2. C R Hebd Seances Acad Sci B 1971;273:388–91.
[40] Clough SA, Beers Y, Klein GP, Rothman LS. Dipole moment of water from Stark measurements of H_2O, HDO, and D_2O. J Chem Phys 1973;59:2254–9.
[41] Camy-Peyret C, Flaud J-M, Guelachvili G, Amiot C. High resolution Fourier transform spectrum of water between 2930 and 4255 cm^{-1}. Mol Phys 1973;26:825–55.
[42] Fleming JW, Gibson MJ. Far-infrared absorption spectra of water vapor $H_2{}^{16}O$ and isotopic modifications. J Mol Spectrosc 1976;62:326–37.
[43] Kauppinen J, Kakkainen T, Kyro E. High-resolution spectrum of water vapour between 30 and 720 cm^{-1}. J Mol Spectrosc 1978;71:15–45.
[44] Papineau N, Camy-Peyret C, Flaud JM, Guelachvili G. The $2v_2$ and v_1 bands of $HD^{16}O$. J Mol Spectrosc 1982;92:451–68.
[45] Bykov AD, Lopasov VP, Makushkin YS, Sinitsa LN, Ulenikov ON, Zuev VE. Rotation–vibration spectra of deuterated water vapor in the 9160–9390 cm^{-1} region. J Mol Spectrosc 1982;94:1–27.
[46] Toth RA, Gupta VD, Brault JW. Line positions and strengths of HDO in the 2400–3300 cm^{-1} region. Appl Opt 1982;21:3337–45.
[47] Guelachvili G. Experimental Doppler-limited spectra of the v_2−bands of $H_2{}^{16}O$, $H_2{}^{17}O$, $H_2{}^{18}O$, and HDO by Fourier-transform spectroscopy—secondary wave-number standards between 1066 and 2296 cm^{-1}. J Opt Soc Am 1983;2:137–50.
[48] Toth RA, Brault JW. Line positions and strengths of lines in the (0 0 1), (1 0 0), and (0 3 0) bands of HDO. Appl Opt 1983;22:908–926.
[49] Messer JK, De Lucia FC, Helminger P. Submillimeter spectroscopy of the major isotopes of water. J Mol Spectrosc 1984;105:139–55.
[50] Bykov AD, Makushkin YS, Serdyukov VI, Sinitsa LN, Ulenikov ON, Ushakova GA. The vibration–rotation HDO absorption spectrum between 8558 and 8774 cm^{-1}. J Mol Spectrosc 1984;105:397–409.
[51] Johns JWC. High-resolution far-infrared (20–350-cm^{-1}) spectra of several isotopic species of H_2O. J Opt Soc Am B 1985;2:1340–54.
[52] Flaud J-M, Camy-Peyret C, Mahmoudi A, Guelachvili G. The v_2 band of $HD^{16}O$. Int J Infrared Millimeter Waves 1986;7:68–76.
[53] Devi VM, Benner DC, Rinsland CP, Smith MAH, Sidney BD. Diode laser measurements of air and nitrogen broadening in the v_2 bands of HDO, $H_2{}^{16}O$, and $H_2{}^{18}O$. J Mol Spectrosc 1986;117:403–7.
[54] Baskakov OI, Alekseev VA, Alekseev EA, Polevoi BI. New submillimeter rotational lines of water and its isotopes. Opt Spectrosc 1987;63:1016–8.
[55] Ohshima T, Sasada H. 1.5-μm DFB semiconductor laser spectroscopy of deuterated water. J Mol Spectrosc 1989;136:250–63.
[56] Bykov AD, Kapitanov VA, Kobtsev SM, Naumenko OV. Detection and analysis of the $5v_3$ absorption band in $HD^{16}O$. Atm Ocean Opt 1990;3:133–41.
[57] Sasada H, Takeuchi S, Iritani M, Nakatani K. Semiconductor-laser heterodyne frequency measurements of 1.52 μm molecular transitions. J Opt Soc Am B 1991;8:713–8.
[58] Rinsland CP, Smith MAH, Devi VM, Benner DC. Measurements of Lorentz-broadening coefficients and pressure-induced line shift coefficients in the v_2 band of $HD^{16}O$. J Mol Spectrosc 1991;150:640–6.
[59] Rinsland CP, Smith MAH, Devi VM, Benner DC. Measurement of Lorentz-broadening coefficients and pressure-induced line-shift coefficients in the v_1 band of $HD^{16}O$ and the v_3 band of $D_2{}^{16}O$. J Mol Spectrosc 1992;156:507–11.
[60] Toth RA. $2v_2-v_2$ and $2v_2$ bands of $H_2{}^{16}O$, $H_2{}^{17}O$, and $H_2{}^{18}O$: line positions and strengths. J Opt Soc Am B 1993;10:1526–44.
[61] Toth RA. $HD^{16}O$, $HD^{18}O$, and $HD^{17}O$ transition frequencies and strengths in the v_2 bands. J Mol Spectrosc 1993;162:20–40.
[62] Goyette TM, Ferguson DW, De Lucia FC, Dutta JM, Jones CR. The pressure broadening of HDO by O_2, N_2, H_2, and He between 100 and 600 K. J Mol Spectrosc 1993;162:366–74.
[63] Paso R, Horneman V-M. High-resolution rotational absorption spectra of $H_2{}^{16}O$, $HD^{16}O$, and $D_2{}^{16}O$ between 110 and 500 cm^{-1}. J Opt Soc Am B 1995;12:1813–38.
[64] Mellau G. ZH2OAES emission spectrum, $P(H_2O)$ = 16.6 Torr, L = 60 cm, T = 1160 K, 1997, Private communication.
[65] Votava O, Fair JR, Plusquellic DF, Riedle E, Nesbitt DJ. High resolution vibrational overtone studies of HOD and H_2O with single mode, injection seeded ring optical parametric oscillators. J Chem Phys 1997;107:8854–6.
[66] Toth RA. Measurement of HDO between 4719 and 5843 cm^{-1}. J Mol Spectrosc 1997;186:276–92.
[67] Toth RA. Line positions and strengths of HDO between 6000 and 7700 cm^{-1}. J Mol Spectrosc 1997;186:66–89.
[68] Lazarev VV, Petrova TM, Sinitsa LN, Zhu Q-S, Han J-X, Hao L-Y. Absorption spectrum of $HD^{16}O$ in 0.7 μm region. Atm Ocean Opt 1998;11:809–12.
[69] Fair JR, Votava O, Nesbitt DJ. OH stretch overtone spectroscopy and transition dipole alignment of HOD. J Chem Phys 1998;108:72–80.
[70] Hu S-M, Lin H, He S-G, Cheng J, Zhu Q-S. Fourier-transform intracavity laser absorption spectroscopy of HOD V_{OD}=5 overtone. Phys Chem Chem Phys 1999;1:3727–30.
[71] Naumenko O, Bertseva E, Campargue A. The 4ν(OH) absorption spectrum of HDO. J Mol Spectrosc 1999;197:122–32.
[72] Toth RA. HDO and D_2O low pressure, long path spectra in the 600–3100 cm^{-1} region; I. HDO line positions and strengths. J Mol Spectrosc 1999;195:73–97.
[73] Naumenko O, Campargue A. High-order resonance interactions in HDO: analysis of the absorption spectrum in the 14 980–15 350 cm^{-1} spectral region. J Mol Spectrosc 2000;199:59–72.
[74] Campargue A, Bertseva E, Naumenko O. The absorption spectrum of HDO in the 16 300–16 670 and 18 000–18 350 cm^{-1} spectral regions. J Mol Spectrosc 2000;204:94–105.
[75] Naumenko O, Bertseva E, Campargue A, Schwenke DW. Experimental and *ab initio* studies of the HDO absorption spectrum in the 13 165–13 500 cm^{-1} spectral region. J Mol Spectrosc 2000;201:297–309.
[76] Siemsen KJ, Bernard JE, Madej AA, Marmet L. Absolute frequency measurement of an HDO absorption line near 1480 cm^{-1}. J Mol Spectrosc 2000;199:144–5.
[77] Hu S-M, Ulenikov ON, Onopenko GA, Bekhtereva ES, He S-G, Wang X-H, et al. High-resolution ro-vibrational spectroscopy of HDO in the region of 7600–8100 cm^{-1}. J Mol Spectrosc 2000;203:228–34.
[78] Bertseva E, Naumenko O, Campargue A. The $5\nu_{OH}$ overtone transition of HDO. J Mol Spectrosc 2000;203:28–36.
[79] Wang X-H, He S-G, Hu S-M, Zheng J-J, Zhu Q-S. Analysis of the HDO absorption spectrum between 9600–10 200 cm^{-1}. Chin Phys 2001;9:885–91.
[80] Jenouvrier A, Mérienne MF, Carleer M, Colin R, Vandaele AC, Bernath PF, et al. The visible and near ultraviolet overtone spectrum of HOD. J Mol Spectrosc 2001;209:165–8.
[81] Ulenikov ON, Hu S-M, Bekhtereva ES, Onopenko GA, Wang XH, He S-G, et al. High-resolution Fourier transform spectrum of HDO in the region 6140–7040 cm^{-1}. J Mol Spectrosc 2001;208:224–35.
[82] Parekunnel T, Bernath PF, Zobov NF, Shirin SV, Polyansky OL, Tennyson J. Emission spectrum of hot HDO in the 380–2190 cm^{-1} region. J Mol Spectrosc 2001;210:28–40.

[83] Hu S-M, He S-G, Zheng J-J, Wang X-H, Ding Y, Zhu Q-S. High-resolution analysis of the $\nu_2+2\nu_3$ band of HDO. Chin Phys 2001;10:1021–7.

[84] Coheur P-F, Fally S, Carleer M, Clerbaux C, Colin R, Jenouvrier A, et al. New water vapor line parameters in the 26 000–13 000 cm^{-1} region. J Quant Spectrosc Radiat Transfer 2002;74:493–510.

[85] Mikhailenko SN, Tyuterev VG, Starikov VI, Albert KK, Winnewisser BP, Winnewisser M, et al. Water spectra in the region 4200–6250 cm^{-1}; extended analysis of $\nu_1+\nu_2$, $\nu_2+\nu_3$, and $3\nu_2$ bands and confirmation of highly excited states from flame spectra and from atmospheric long-path observations. J Mol Spectrosc 2002;213:91–121.

[86] Janca A, Tereszchuk K, Bernath PF, Zobov NF, Shirin SV, Polyansky OL, et al. Emission spectrum of hot HDO below 4000 cm^{-1}. J Mol Spectrosc 2003;219:132–5.

[87] Bertseva E, Naumenko OV, Campargue A. The absorption spectrum of HDO around 1.0 μm by ICLAS-VECSEL. J Mol Spectrosc 2003;221:38–46.

[88] Mérienne MF, Jenouvrier A, Hermans C, Vandaele AC, Carleer M, Clerbaux C, et al. Water vapor line parameters in the 13 000–9250 cm^{-1} region. J Quant Spectrosc Radiat Transfer 2003;82:92–117.

[89] Naumenko OV, Hu SM, He S-G, Campargue A. Rovibrational analysis of the absorption spectrum of HDO between 10 110 and 12 215 cm^{-1}. Phys Chem Chem Phys 2004;6:910–8.

[90] Naumenko OV, Voronina S, Hu S-M. High resolution Fourier transform spectrum of HDO in the 7500–8200 cm^{-1} region: revisited. J Mol Spectrosc 2004;227:151–7.

[91] Macko P, Romanini D, Mikhailenko SN, Naumenko OV, Kassi S, Jenouvrier A, et al. High sensitivity CW-cavity ring down spectroscopy of water in the region of the 1.5 μm atmospheric window. J Mol Spectrosc 2004;227:90–108.

[92] Tolchenov RN, Tennyson J. Water line parameters for weak lines in the range 7400–9600 cm^{-1}. J Mol Spectrosc 2005;231:23–7.

[93] Tolchenov RN, Zobov NF, Shirin SV, Polyansky OL, Tennyson J, Naumenko O, et al. Water vapor line assignments in the 9250–26 000 cm^{-1} frequency range. J Mol Spectrosc 2005;233:68–76.

[94] Bach M, Fally S, Coheur P-F, Carleer M, Jenouvrier A, Vandaele AC. Line parameters of HDO from high-resolution Fourier transform spectroscopy in the 11 500–23 000 cm^{-1} spectral region. J Mol Spectrosc 2005;232:341–50.

[95] Ulenikov ON, Hu S-M, Bekhtereva ES, Zhu Q-S. High-resolution rovibrational spectroscopy of HDO in the region of 8900–9600 cm^{-1}. J Mol Spectrosc 2005;231:57–65.

[96] Campargue A, Vasilenko I, Naumenko O. Intracavity laser absorption spectroscopy of HDO between 11 645 and 12 330 cm^{-1}. J Mol Spectrosc 2005;234:216–27.

[97] Theule P, Callegari A, Rizzo TR, Muenter JS. Dipole moments of HDO in highly excited vibrational states measured by Stark induced photofragment quantum beat spectroscopy. J Chem Phys 2005;122:124312.

[98] Naumenko OV, Leshchishina O, Campargue A. High sensitivity absorption spectroscopy of HDO by ICLAS-VeCSEL between 9100 and 9640 cm^{-1}. J Mol Spectrosc 2006;236:58–69.

[99] Joly L, Parvitte B, Zéninari V, Courtois D, Durry G. A spectroscopic study of water vapor isotopologues $H_2{}^{16}O$, $H_2{}^{18}O$ and HDO using a continuous wave DFB quantum cascade laser in the 6.7 μm region for atmospheric applications. J Quant Spectrosc Radiat Transfer 2006;102:129–38.

[100] Voronin BA, Naumenko OV, Tolchenov RN, Tennyson J, Fally S, Coheur P-F, et al. HDO absorption spectrum above 11 500 cm^{-1}: assignment and dynamics. J Mol Spectrosc 2007;244:87–101.

[101] Jenouvrier A, Daumont L, Régalia-Jarlot L, Tyuterev VG, Carleer M, Vandaele AC, et al. Fourier transform measurements of water vapor line parameters in the 4200–6600 cm^{-1} region. J Quant Spectrosc Radiat Transfer 2007;105:326–55.

[102] Mazzotti F, Tolchenov RN, Campargue A. High sensitivity ICLAS of $H_2{}^{18}O$ in the region of the second decade (11 520–12 810 cm^{-1}). J Mol Spectrosc 2007;243:78–89.

[103] Mikhailenko SN, Wang L, Kassi S, Campargue A. Weak water absorption lines around 1.455 and 1.66 μm by CW-CRDS. J Mol Spectrosc 2007;244:170–8.

[104] Naumenko OV, Voronin BA, Mazzotti F, Tennyson J, Campargue A. Intracavity laser absorption spectroscopy of HDO between 12 145 and 13 160 cm^{-1}. J Mol Spectrosc 2008;248:122–33.

[105] Lisak D, Hodges JT. Low-uncertainty H_2O line intensities for the 930-nm region. J Mol Spectrosc 2008;249:6–13.

[106] Petrova TM, Sinitsa LN, Solodov AM. H_2O lines shifts measurements in 1.06 μm region. SPIE 2008;6936:93602.

[107] Tolchenov RN, Tennyson J. Water line parameters from refitted spectra constrained by empirical upper state levels: study of the 9500–14 500 cm^{-1} region. J Quant Spectrosc Radiat Transfer 2008;109:559–68.

[108] Liu A, Naumenko O, Kassi S, Campargue A. High sensitivity CW-CRDS of ^{18}O enriched water near 1.6 μm. J Quant Spectrosc Radiat Transfer 2009;110:1781–800.

[109] Naumenko OV, Beguier S, Leshchishina OM, Campargue A. ICLAS of HDO between 13 020 and 14 115 cm^{-1}. J Quant Spectrosc Radiat Transfer 2010;111:36–44.

[110] Lovas FJ. Microwave spectral tables. II. Triatomic molecules. J Phys Chem Ref Data 1978;7:1445–750.

[111] Stevenson MJ, Townes CH. Quadrupole moment of ^{17}O. Phys Rev 1957;107:635–7.

[112] Zelinger Z, Barret B, Kubát P, Ricaud P, Attie J-L, Flochmoën EL, et al. Observation of $HD^{18}O$, CH_3OH and vibrationally-excited N_2O from Odin/SMR measurements. Mol Phys 2006;104:2815–20.

[113] Toth RA. Measurements of line positions and strengths of $HD^{18}O$ and $D_2{}^{18}O$ in the 2500–4280 cm^{-1} region. J Mol Struct 2005;742:49–68.

[114] Mikhailenko SN, Tashkun SA, Putilova TA, Starikova EN, Daumont L, Jenouvrier A, et al. Critical evaluation of measured rotation–vibration transitions and an experimental dataset of energy levels of $HD^{18}O$. J Quant Spectrosc Radiat Transfer 2009;110:597–608.

[115] Mikhailenko SN, Tashkun SA, Daumont L, Jenouvrier A, Fally S, Vandaele AC, et al. Line positions and energy levels of the ^{18}O substitutions from the HDO/D_2O spectra between 5600 and 8800 cm^{-1}. J Quant Spectrosc Radiat Transfer, 2010, doi:10.1016/j.jqsrt.2010.01.028.

[116] Partridge H, Schwenke DW. The determination of an accurate isotope dependent potential energy surface for water from extensive ab initio calculations and experimental data. J Chem Phys 1997;106:4618–39.

[117] Mátyus E, Fábri C, Szidarovszky T, Czakó G, Allen WD, Császár AG. Assigning quantum labels to variationally computed rotational–vibrational eigenstates. J Chem Phys, 2010, doi:10.1063/1.3451075.

[118] Voronin BA, Tolchenov RN, Tennyson J, Lugovskoy AA, Yurchenko SN. A high accuracy computed line list for the HDO molecule. Mon Not R Astr Soc 2009;402:492–6.

[119] Yurchenko SN, Voronin BA, Tolchenov RN, Doss N, Naumenko OV, Thiel W, et al. Potential energy surface of HDO up to 25 000 cm^{-1}. J Chem Phys 2008;128:044312.

[120] Lodi L, Tolchenov RN, Tennyson J, Lynas-Gray AE, Shirin SV, Zobov NF, et al. A high accuracy dipole surface for water. J Chem Phys 2008;128:044304.

[121] Tennyson J, Kostin MA, Barletta P, Harris GJ, Ramanlal J, Polyansky OL, et al. DVR3D: a program suite for the calculation of rotation–vibration spectra of triatomic molecules. Comput Phys Commun 2004;163:85–116.

[122] Polyansky OL, Zobov NF, Viti S, Tennyson J, Bernath PF, Wallace L. K band spectrum of water in sunspots. Astrophys J 1997;489:L205–8.

[123] Bykov A, Naumenko O, Sinitsa L, Voronin B, Camy-Peyret J-MFC, Lanquetin RA. High-order resonances in the water molecule. J Mol Spectrosc 2001;205:1–8.

[124] Freed C, Odonnell RG, Ross AHM. Absolute frequency calibration of CO_2 isotope laser transitions. IEEE Trans Instrum Meas 1976;25:431–7.

[125] Knight DJE, Edwards GJ, Pearce PR, Cross NR. Measurement of the frequency of the 3.39-μm methane-stabilized laser to ± 3 parts in 10^{11}. IEEE Trans Instrum Meas 1980;29:257–64.

[126] Pollock CR, Petersen FR, Jennings DA, Wells JS, Maki AG. Absolute frequency measurements of the 2–0 band at CO at 2.3 μm; calibration standard frequencies from high resolution color center laser spectroscopy. J Mol Spectrosc 1983;99:357–68.

[127] Brown LR, Toth RA. Comparisons of the frequencies of NH_3, CO_2, H_2O, N_2O and CH_4 as infrared calibration standards. J Opt Soc Am B 1985;2:842–56.

[128] Nakagawa K, deLabachelerie M, Awaji Y, Kourogi M. Accurate optical frequency atlas of the 1.5 μm bands of acetylene. J Opt Soc Am B 1996;13:842–56.

[129] Falke S, Tiemann E, Lisdat C, Schnatz H, Grosche G. Transition frequencies of the D lines of ^{39}K, ^{40}K and ^{41}K measured with a femtosecond laser frequency comb. Phys Rev A 2006;149:032503.

[130] Guelachvili G, Birk M, Bordé CJ, Brault JW, Brown LR, Carli B, et al. High resolution wavenumber standards for the infrared. J Mol Spectrosc 1996;177:164–79.

[131] Maki A, Wells J. New wave-number calibration tables from heterodyne frequency measurements. J Res Nat Inst Stand Technol 1992;97:409–70.
[132] Rothman LS, Gamache RR, Goldman A, Brown LR, Toth RA, Pickett HM, et al. The *HITRAN* database—1986 edition. Appl Opt 1987;26:4058–97.
[133] Guelachvili G. Absolute wavenumbers and molecular constants of the fundamental bands of $^{12}C^{16}O$, $^{12}C^{17}O$, $^{12}C^{18}O$, $^{13}C^{16}O$, $^{13}C^{18}O$ and of the 2-1 bands of $^{12}C^{16}O$ and $^{13}C^{16}O$ around 5 μm by Fourier spectroscopy under vacuum. J Mol Spectrosc 1979;75:251–69.
[134] Sasada H, Yamada K. Calibration lines of HCN in the 1.5 μm region. Appl Opt 1990;29:3535–47.
[135] Toth RA. Measurement of $H_2{}^{16}O$ line positions and strengths—11 610 to 12 861 cm^{-1}. J Mol Spectrosc 1994;116:176–83.
[136] Schermaul R, Brault JW, Canas AAD, Learner RCM, Polyansky OL, Zobov NF, et al. Weak line water vapour spectrum in the regions 13 200–15 000 cm^{-1}. J Mol Spectrosc 2002;211:169–78.
[137] Schermaul R, Learner RCM, Newnham DA, Williams RG, Ballard J, Zobov NF, et al. The water vapour spectrum in the region 8600–15 000 cm^{-1}: experimental and theoretical studies for a new spectral line database i: laboratory measurements. J Mol Spectrosc 2001;208:32–42.
[138] Liu AW, Du JH, Song KF, Wang L, Wan L, Hu SM. High-resolution Fourier-transform spectroscopy of ^{18}O-enriched water molecule in the 1080–7800 cm^{-1} region. J Mol Spectrosc 2006;237:149–62.
[139] Messer JK, De Lucia FC, Helminger P. The pure rotational spectrum of water-vapor—a millimeter, submillimeter and far infrared analysis. Int J Infrared Millimeter Waves 1983;4:505–39.
[140] Schwenke DW, Partridge H. Convergence testing of the analytic representation of an ab initio dipole moment function for water: improved fitting yields improved intensities. J Chem Phys 2000;113:6592–7.
[141] Rothman LS, Gordon IE, Barbe A, Benner DC, Bernath PF, Birk M, et al. The *HITRAN* 2008 molecular spectroscopic database. J Quant Spectrosc Radiat Transfer 2009;110:533–72.
[142] Rothman LS, Jacquemart D, Barbe A, Benner DC, Birk M, Brown LR, et al. The *HITRAN* 2004 molecular spectroscopic database. J Quant Spectrosc Radiat Transfer 2005;96:139–204.
[143] Pickett HM, Poynter RL, Cohen EA, Delitsky ML, Pearson JC, Müller HSP. Submillimeter, millimeter, and microwave spectral line catalog. J Quant Spectrosc Radiat Transfer 1998;60:883–90.
[144] Toth RA. SISAM database 〈http://mark4sun.jpl.nasa.gov〉, 2007.
[145] JPL catalog. URL 〈http://spec.jpl.nasa.gov/ftp/pub/catalog/catdir.html〉.
[146] Lodi L, Tennyson J. A linelist of allowed and forbidden rotational transitions for water. J Quant Spectrosc Radiat Transfer 2008;109:1219–33.
[147] Lisak D, Havey DK, Hodges JT. Spectroscopic line parameters of water vapor for rotation–vibration transitions near 7180 cm^{-1}. Phys Rev A 2009;79:052507.
[148] Bykov AD, Fazliev AZ, Filippov NN, Kozodoev AV, Privezentsev AI, Sinitsa LN, et al. Distributed information system on atmospheric spectroscopy. Geophysical Research Abstracts, vol. 9, 01906, SRef-ID: 1607-7962/gra/EGU2007-A-01906, 2007.
[149] Császár AG, Fazliev AZ, Tennyson J. W@DIS—Prototype information system for systematization of spectral data of water. In: Abstracts of the twentieth colloquium on high resolution molecular spectroscopy, Dijon, France 〈http://vesta.u-bourgogne.fr/hrms/〉, 2007.
[150] Guelachvili G, Rao KN. Handbook of infrared standards. Orlando, FL: Academic Press; 1986.
[151] Puzzarini C, Cazzoli G, Harding ME, Vázquez J, Gauss J. A new experimental absolute nuclear magnetic shielding scale for oxygen based on the rotational hyperfine structure of $H_2{}^{17}O$. J Chem Phys 2009;131:234304.